Spatial Period-Doubling Agglomeration of a Core-Periphery Model with a System of Cities

Ikeda, Kiyohiro and Akamatsu, Takashi and Kono, Tatsuhito

Department of Civil and Environmental Engineering, Tohoku University

18 February 2009

Spatial Period-Doubling Agglomeration of a Core–Periphery Model with a System of Cities*

Kiyohiro Ikeda†,
Takashi Akamatsu and Tatsuhito Kono‡

February 18, 2009

Abstract

The orientation and progress of spatial agglomeration for Krugman's core–periphery model are investigated in this paper. Possible agglomeration patterns for a system of cities spread uniformly on a circle are set forth theoretically. For example, a possible and most likely course predicted for eight cities is a gradual and successive one—concentration into four cities and then into two cities en route to a single city. The existence of this course is ensured by numerical simulation for the model. Such gradual and successive agglomeration, which is called spatial-period doubling, presents a sharp contrast with the agglomeration of two cities, for which spontaneous concentration to a single city is observed in models of various kinds. It exercises caution about the adequacy of the two cities as a platform of the spatial agglomerations and demonstrates the need of the study on a system of cities.

Keywords: Agglomeration of population, Bifurcation, Core–periphery model, Group theory, Spatial period doubling

JEL classification: F12; O18; R12

*This research was supported by JSPS grants 19360227 and 21360240.

†Address for correspondence: Kiyohiro Ikeda, Department of Civil and Environmental Engineering, Tohoku University, Aoba 6-6-06, Sendai 980-8579, Japan; ikeda@civil.tohoku.ac.jp.

‡Graduate School of Information Sciences, Tohoku University Aoba 6-6-06, Sendai 980-8579, Japan

1 Introduction

Emergence of the spatial economic agglomeration attributable to market interactions has attracted much attention of spatial economists and geographers. Among the many descriptions available in the literature, the core–periphery model of Krugman (1991) [18] is touted as the first and the most successful attempt to clarify the microeconomic underpinning of the spatial economic agglomeration in a full-fledged general equilibrium approach[1]. The core–periphery model introduced the Dixit–Stiglitz (1977) [6] model of monopolistic competition into spatial economics and provided a new framework to explain interactions that occur among increasing returns at the level of firms, transportation costs, and factor mobility. Such a framework paved the way for development of the New Economic Geography[2] as a mainstream field of economics. Furthermore, in recent years, the framework has been applied to various policy issues in areas such as trade policy, taxation, and macroeconomic growth analysis (Baldwin et al., 2003 [1]).

Yet most reports of the literature in New Economic Geography have remained confined to two-city models in which spatial economic concentration to a single city is triggered by bifurcation[3]. The two-city model is the most pertinent starting point by virtue of its analytical tractability, but it has a limited capability to express spatial effects. In reality, economic agglomerations can take place in more than two locations, as evidenced by results of several empirical studies. For example, Behrens and Thisse (2007) [2] stated that "Among a system of cities, indirect spatial effects emerge and complicate the analysis. Dealing with these spatial indeterminacies constitutes a

[1]This is based on an appraisal by Fujita and Thisse (2009) [12] in honor of Krugman's 2008 Nobel Memorial Prize in Economic Sciences.

[2]Comprehensive reviews of the NEG models are available in a survey by Ottaviano and Puga (1998) [24], in a review by Fujita and Thisse (2009) [12], and in several books as follows: Fujita et al. (1999) [10], Brakman et al., 2001 [3], Fujita and Thisse (2002) [11], Baldwin et al. (2003) [1], Henderson and Thisse (2004) [15], Combes et al. (2008) [4], and Glaeser (2008) [13].

[3]The two identical symmetric cities are in a stable state with high transport costs. When the costs are reduced to a certain level, tomahawk bifurcation triggers a spontaneous concentration to a single city by breaking the symmetry (e.g., Krugman, 1991 [18], Fujita et al., 1999 [10], Forslid and Ottaviano, 2003 [9]).

main theoretical and empirical challenge NEG and regional economics must surely confront in the future[4]." We must analyze a system of cities thoroughly in careful comparison with the two-city model to answer the question, "To what degree can we extrapolate the predictions and implications derived from two-city analysis to a system of cities?"

Several reports in the literature have described attempts to transcend the two-city special case with a local analysis (linearized eigenproblem) of the racetrack economy[5]. Krugman (1993 [19], 1996 [20]) identified the emergence of several spatial frequencies. Yet, currently, it is difficult analytically to extract agglomeration properties from the nonlinear equations of core–periphery models with an arbitrary discrete number of cities.

Numerical simulations might be effective for identifying agglomeration patterns for a system of cities. A numerical simulation on 12 symmetric cities of equal size is conducted to observe that the symmetric equilibrium often becomes unstable (cf., Krugman, 1991 [18]). Fujita et al. (1999) [10] obtained post-bifurcation equilibria for three cities. Nevertheless, it seems premature to infer a global view of agglomeration based on currently available numerical information. A naive numerical simulation for an increased number of cities must address a rapidly increasing numerical information and might therefore not be very promising.

The objective of this paper is to investigate the orientation and progress of agglomerations of a system of cities and, in turn, to test the adequacy of the two-city model as a spatial platform. Possible agglomeration patterns and courses of the pattern change of a racetrack economy for the multi-regional core–periphery model[6] are obtained using group-theoretic bifurcation the-

[4]The difficulty encountered in solving the dimensionality problem is reminiscent of the n-body problem in mechanics, which is solved for $n = 2$ but not for an arbitrary number of bodies.

[5]The racetrack economy uses a system of identical cities that spread uniformly around the circumference of a circle. See, e.g., Krugman (1993) [19], 1996 [20], Fujita et al. (1999) [10], Picard and Tabuchi (2009) [26].

[6]The core–periphery model with n cities is presented in §2 as a recapitulation and a reorganization of Krugman (1991) [18] and Fujita et al. (1999, Chapter 5) [10]. This model uses a spatial version of the Dixit–Stiglitz model, considers an economy with two sectors—agriculture and manufacturing— and assumes an upper-tier utility function of the Cobb–Douglas type with CES sub-preferences over manufacturing varieties.

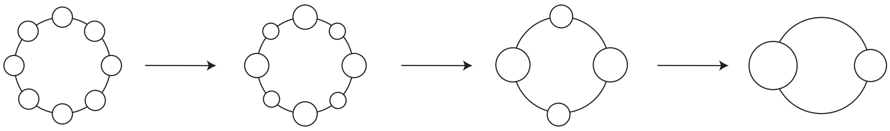

Figure 1: Spatial period-doubling cascade for the eight cities (area of ◯ denotes the size of the associated city: the arrow denotes the occurrence of a bifurcation)

ory[7]. A possible and the most likely course of agglomeration predicted is *spatial period-doubling cascade* (cf. Proposition 5 in §5.4). An example of this cascade is shown for eight cities in Fig. 1, in which the area of the circle represents the population of the associated city and the arrow indicates the occurrence of a bifurcation[8]. A system of $2^3 = 8$ identical cities (for some positive integer k) concentrates into $2^2 = 4$ identical larger cities, en route to the concentration to the single megalopolis. Consequently, the concentration progresses successively in association with the doubling of the spatial period.

The validity of the theoretical prediction is assessed using numerical simulation. Basic equations of the core-periphery model are rewritten to be compatible with computational bifurcation theory[9] (cf. §3). A combination[10] of the group-theoretic bifurcation theory and the computational bifurcation theory is vital in the numerical simulation of the agglomerations of a racetrack economy with many cities.

Although Krugman's (1993 [19], 1996 [20]) analysis of the racetrack economy gives the orientation of the breaking of uniformity, we study the progress of agglomerations thereafter, as well as the orientation. The possible equilibrium and associated agglomeration patterns of 4, 6, 8, and 16 cities are studied theoretically (cf. §5) and are obtained numerically (cf. §6) in an exhaustive manner, while only a few were found and studied in the previous numerical simulations. Results show that the racetrack economy among a

[7]The major framework of this theory has already been developed in physical fields (see, e.g., Golubitsky et al., 1988 [14]; Ikeda and Murota, 2002 [16]), and is introduced into §4. This theory is reorganized to be applicable to the core–periphery model in §5.

[8]See §5.4 for the precise meaning of this figure.

[9]See, e.g., Crisfield (1977) [5] for an explanation of this theory.

[10]The group-theoretic bifurcation theory represents a map and the computational bifurcation theory represents a car in the tracing of complex equilibria. See, e.g., Ikeda and Murota, 2002 [16] for successful combinatory use of these two theories.

system of cities, for the same value of transport cost, has increasing numbers of stable equilibria when the number of cities increases. Such an increase of stable equilibria is a fundamental difficulty that might instill pessimism about the usefulness of the bifurcation analysis of the racetrack economy. Nonetheless, as the most likely course of agglomerations of a system of cities, the spatial period doubling cascade for 4, 8, and 16 cities is actually found through numerical simulation, and thereby supports that pessimistic view.

This paper is organized as follows. The core–periphery model is introduced into §2. Governing equations are presented with a study of stability in §3. A brief explanation of group-theoretic bifurcation theory is offered in §4. Bifurcation theory of the racetrack economy is described in §5. Agglomerations of the racetrack economy with a system of cities are investigated in §6. The Appendix offers theoretical details and proofs.

2 Core–periphery model

A core–periphery model with an arbitrary discrete number of cities is presented as a recapitulation and a reorganization of Krugman (1991) [18] and Fujita et al. (1999, Chapter 5) [10]. The economy comprises n possible locations (labeled $i = 1, \ldots, n$) around a circumference of a racetrack, two industrial sectors (agriculture and manufacture), and two factors of production (agricultural labor and manufacturing labor). The agricultural sector is perfectly competitive and produces a homogeneous good, whereas the manufacturing sector is imperfectly competitive with increasing returns, producing various and differentiated goods. Manufacturing laborers are mobile across locations, but agricultural laborers are immobile. Laborers of each type consume two goods and supply one unit of labor inelastically. The utility functions are identical for agricultural labor and manufacturing labor. The equilibrium of the model is determined through two stages: the short-run equilibrium and the long-run equilibrium. The short-run equilibrium is determined according to the spatial allocation of manufacturing workers. In the long-run equilibrium, manufacturing workers can migrate to a city with a higher real wage. As a result of such manufacturing workers' migration, the spatial allocation of manufacturing workers is determined.

2.1 Short-run equilibrium

The short-run equilibrium determines the income of each city, the price index of manufactures in that city, the wage rate of workers in that city, and the real wage rate in that city given the spatial allocation of manufacturing laborers determined by the long-run equilibrium.

The nominal wage rate w_i for the manufacturing labor force of the ith city is given as

$$w_i = [\sum_{j=1}^{n} Y_j t_{ij}^{1-\sigma} G_j^{\sigma-1}]^{1/\sigma}, \quad (i = 1, \ldots, n); \tag{1}$$

the manufactured price index for the ith city is given as

$$G_i = [\sum_{j=1}^{n} \lambda_j (w_j t_{ij})^{1-\sigma}]^{1/(1-\sigma)}, \quad (i = 1, \ldots, n). \tag{2}$$

Here Y_i signifies the total income for the ith city, t_{ij} denotes the transport cost in terms of the amount of the manufactured good dispatched per unit received, σ stands for the elasticity of substitution between differentiated goods, G_i denotes the manufactured price index, and λ_i $(i = 1, \dots, n)$ stands for the ratio of the manufacturing labor force for the ith city to the whole manufacturing force, which is called the population of the ith city for short.

The total income for the ith city is expressed as

$$Y_i = \mu \lambda_i w_i + (1 - \mu)/n, \quad (i = 1, \dots, n), \tag{3}$$

assuming that the agricultural wage has unity as a numéraire, where μ is the ratio of the manufacturing labor force, the first term $\mu \lambda_i w_i$ in the right-hand-side of (3) is the income of the manufacturing labor force, and the second term $(1 - \mu)/n$ is that of the agricultural one.

2.2 Long-run equilibrium

In the long-run equilibrium, the manufacturing workers are assumed to migrate to a city with a higher real wage. We express the real wage ω_i of the ith city as

$$\omega_i = w_i G_i^{-\mu}, \quad (i = 1, \dots, n), \tag{4}$$

and consider the highest equilibrium real wage $\bar{\omega}$.

The long-run equilibrium employs the complementarity condition

$$\begin{cases} \omega_i - \bar{\omega} = 0, & (\lambda_i > 0), \\ \omega_i - \bar{\omega} \leq 0, & (\lambda_i = 0), \end{cases} \tag{5}$$

$(i = 1, \dots, n)$ and the conservation law of population

$$\sum_{i=1}^{n} \lambda_i = 1. \tag{6}$$

2.3 Iceberg transport costs

We employ the iceberg form of transport costs and define them as follows.

Assumption 1 (Iceberg transport costs). For the racetrack economy on a circle with the unit radius, which is studied in this paper, we define the transport cost t_{ij} between the two cities i and j by

$$t_{ij} = \exp(\tau D_{ij}), \quad (i, j = 1, \ldots, n), \tag{7}$$

where τ is the transport parameter and

$$D_{ij} = \frac{2\pi}{n} \min(|i-j|, n - |i-j|), \quad (i, j = 1, \ldots, n)$$

represents the shortest distance between cities i and j; $\min(\cdot, \cdot)$ denotes the smaller value of the variables in parentheses.

3 Governing equations and stability

We have presented a set of equations for the core–periphery model in §2. From these equations, we derive a system of nonlinear governing equations of the model and derive the stability condition of the solutions of the model in a manner suitable for the theoretical analysis of the racetrack economy in §5 and the numerical analysis in §6. In the derivation of the governing equations, the condensation is conducted on the set of equations to suppress auxiliary equations and variables in §3.1. The stability condition is formulated in terms of the eigenanalysis of a Jacobian matrix of the governing equations in §3.2.

3.1 Governing equations

Among many variables and parameters of these equations, we regard $\boldsymbol{\lambda} = (\lambda_1, \ldots, \lambda_n)^\top$ as an independent variable vector and τ as a bifurcation parameter[11], and condense[12] other variables as below.

The real wage in (4) can be expressed from (1)–(3) and (7) as a function of $(\boldsymbol{\lambda}, \tau)$ as

$$\omega_i = \omega_i(\boldsymbol{\lambda}, \tau), \quad (i = 1, \ldots, n). \tag{8}$$

The highest equilibrium real wage among the cities can be expressed from (5), (6), and (8) as a function of $(\boldsymbol{\lambda}, \tau)$ as

$$\bar{\omega} = \bar{\omega}(\boldsymbol{\lambda}, \tau). \tag{9}$$

We express a system of governing equations for the model as

$$\boldsymbol{F}(\boldsymbol{\lambda}, \tau) \;=\; \begin{pmatrix} \{\omega_1(\boldsymbol{\lambda}, \tau) - \bar{\omega}(\boldsymbol{\lambda}, \tau)\}\lambda_1 \\ \vdots \\ \{\omega_n(\boldsymbol{\lambda}, \tau) - \bar{\omega}(\boldsymbol{\lambda}, \tau)\}\lambda_n \end{pmatrix} = \boldsymbol{0}, \tag{10}$$

[11] μ and σ are regarded as auxiliary parameters that are pre-specified for each problem.

[12] A numerical counterpart of the condensation of the variables that is used in the numerical bifurcation analysis in §6 is presented in Appendix A.

$$
\boldsymbol{G}(\boldsymbol{\lambda}, \tau) \quad = \quad \begin{pmatrix} -\{\omega_1(\boldsymbol{\lambda}, \tau) - \bar{\omega}(\boldsymbol{\lambda}, \tau)\} \\ \vdots \\ -\{\omega_n(\boldsymbol{\lambda}, \tau) - \bar{\omega}(\boldsymbol{\lambda}, \tau)\} \\ \lambda_1 \\ \vdots \\ \lambda_n \end{pmatrix} \geq \mathbf{0} \qquad (11)
$$

from (5) with (8) and (9).

Assumption 2 (Smoothness). $\boldsymbol{F}$ and $\boldsymbol{G}$ are sufficiently smooth functions.

Remark 1 The equality (10) is formulated as a special form in that λ_i is multiplied to the ith component $\omega_i(\boldsymbol{\lambda}, \tau) - \bar{\omega}(\boldsymbol{\lambda}, \tau)$ of (5). This special form is pertinent to the discussion of asymptotic stability in §3.2 and of the study of bifurcation in Appendix D.

Although there are variety of strategies[13] to solve the equality (10) and inequality (11) simultaneously, in favor of the consistency with bifurcation theory, we use the following two-step strategy.

- Step 1: Obtain a family of solutions (equilibrium points) $(\boldsymbol{\lambda}, \tau)$ of (10) that forms smooth equilibrium path(s). A nonlinear system undergoing bifurcation involves several sets of equilibrium paths, including bifurcated paths.

- Step 2: Among the equilibrium paths, we extract only those satisfying the inequality (11), i.e., *sustainable solutions* $(\omega_i(\boldsymbol{\lambda}, \tau) - \bar{\omega}(\boldsymbol{\lambda}, \tau) \leq 0)$ with non-negative populations $(\lambda_i \geq 0)$ $(i = 1, \ldots, n)$.

[13]The variational inequality approach, for example, is known as a strategy to tackle such problems (e.g. Nagurney, 1993 [23]; Facchinei and Pang, 2003 [7]).

3.2 Stability and economical feasibility of solutions

We introduce a local stability condition[14] based on the dynamics[15]

$$\frac{d\boldsymbol{\lambda}}{dt} = \boldsymbol{F}(\boldsymbol{\lambda}, \tau). \tag{12}$$

If all eigenvalues e_i $(i = 1, \cdots, n)$ of the Jacobian matrix of $\boldsymbol{F}$,

$$J(\boldsymbol{\lambda}, \tau) = \frac{\partial \boldsymbol{F}}{\partial \boldsymbol{\lambda}},$$

have negative real parts at a solution $(\boldsymbol{\lambda}, \tau)$, then the solution is linearly stable, and is asymptotically stable as $t \to \infty$. If at least one eigenvalue has a positive real part, then the solution is linearly unstable, and is asymptotically unstable as $t \to \infty$.

In practice, we are interested in solutions that are stable and satisfy the inequality (11) and call such solutions (economically) *feasible* solutions. Solutions which are not feasible are called (economically) *infeasible* solutions, which include:

- unstable solutions for which e_i for some i has a positive real part,
- solutions with negative population $\lambda_i < 0$ for some i, and/or
- *unsustainable solutions* with $\omega_i - \bar{\omega} > 0$ $(\lambda_i = 0)$ for some i.

Proposition 1 below is pertinent in the check of feasibility.

Proposition 1 *The feasibility of a solution $(\boldsymbol{\lambda}, \tau)$ that satisfies the equality condition (10) with non-negative populations $\lambda_i \geq 0$ $(i = 1, \ldots, n)$ is classifiable as follows:*

i) The solution is feasible if all eigenvalues e_i $(i = 1, \ldots, n)$ of $J(\boldsymbol{\lambda}, \tau)$ have negative real parts.

ii) The solution is infeasible if an eigenvalue(s) has a positive real part(s).

Proof. See Appendix C. □

[14]The present stability condition is based on the asymptotic stability (e.g., Lorenz, 1997 [21]; Ikeda and Murota, 2002 [16]).

[15]The dynamics in (12) corresponds to the replicator dynamics (cf. Fujita et al. 1999, [10]).

4 Group-theoretic bifurcation theory

The break bifurcation[16] is explained in light of group-theoretic bifurcation theory. This theory, a standard means to describe the bifurcation of symmetric systems, has been developed to obtain the rules of pattern formation—emergence of solutions with reduced symmetries via so-called symmetry-breaking bifurcations (cf. Golubitsky et al., 1988 [14]). This theory will be employed to investigate possible bifurcations of the racetrack economy in §5.

We are interested in a symmetric system that satisfies the symmetry condition, called the equivariance[17]

$$T(g)\boldsymbol{F}(\boldsymbol{\lambda}, \tau) = \boldsymbol{F}(T(g)\boldsymbol{\lambda}, \tau), \quad g \in G \tag{13}$$

of $\boldsymbol{F}(\boldsymbol{\lambda}, \tau)$ to a symmetry group G in terms of an $n \times n$ orthogonal matrix representation $T(g)$ of G that expresses the geometrical transformation for an element g of G.

The Jacobian matrix $J(\boldsymbol{\lambda}, \tau)$ is endowed with the symmetry condition

$$T(g)J(\boldsymbol{\lambda}, \tau) = J(\boldsymbol{\lambda}, \tau)T(g), \quad g \in G \tag{14}$$

if $\boldsymbol{\lambda}$ is G-symmetric in the sense that $T(g)\boldsymbol{\lambda} = \boldsymbol{\lambda}$ $(g \in G)$. By virtue of (14), it is possible to construct a transformation matrix H, the column vectors of which are made up of discrete Fourier series (cf. Murota and Ikeda, 1991 [22]), such that the Jacobian matrix J is transformed into a block-diagonal form:

$$\tilde{J} = H^\top J H = \begin{pmatrix} \tilde{J}^0 & & O \\ & \tilde{J}^1 & \\ O & & \ddots \end{pmatrix} \tag{15}$$

with diagonal block matrices $\tilde{J}^k$ $(k = 0, 1, \ldots)$. A diagonal block, say $\tilde{J}^0$, has G-symmetric eigenvectors, while eigenvectors of other blocks $\tilde{J}^k$ $(k = 1, 2, \ldots)$ have reduced symmetries labeled by subgroups G_k $(k = 1, 2, \ldots)$

[16] See Appendix B.4 for the explanation of break bifurcation.

[17] The equivariance (13) is not an artificial condition for mathematical convenience, but a natural consequence of the objectivity of the equation: the observer-independence of the mathematical description.

of G. This is a mechanism to engender symmetry breaking via bifurcation. This block-diagonal form is suitable for an analytical eigenanalysis of the Jacobian matrix (cf. §5.3).

The bifurcation of a symmetric system with the equivariance (13) has been studied in group-theoretic bifurcation theory and has properties (cf. Ikeda and Murota, 2002 [16]):

- Property 1: The symmetry of the equilibrium points is preserved until branching into a bifurcated path.

- Property 2: In association with repeated bifurcations, one can find a hierarchy of subgroups

$$G \longrightarrow G_1 \longrightarrow G_2 \longrightarrow \cdots \tag{16}$$

  that characterizes the hierarchical change of symmetries. Here $\longrightarrow$ denotes the occurrence of break bifurcation.

- Property 3: A bifurcated path sometimes regains symmetry on a bifurcation point on another equilibrium path with a higher symmetry.

In this section, the bifurcation rule is described in such a sequence that the symmetry is reduced successively via bifurcations. However, when we observe some economic system by decreasing the transport cost monotonously from ∞ to 0, a bifurcated path sometimes regains symmetry at a bifurcation point as explained in Property 3 presented above.

5 Bifurcation of a racetrack economy

The tomahawk bifurcation of Krugman's core–periphery model with two cities is well known to produce spontaneous concentration to a single city. In contrast, it will be demonstrated in §6 that the racetrack economy of a system of cities displays more complex bifurcation. The objective of this section is to investigate such bifurcation by group-theoretic bifurcation theory presented in §4. We present several theoretical developments that will be employed in the analysis of the racetrack economy in §6:

- Symmetry of the racetrack economy and its governing equation are illustrated in §5.1.
- Trivial solutions[18] of the racetrack economy are determined in view of the symmetry in §5.2.
- Possible bifurcated solutions and possible courses of bifurcations from the uniform population solution are investigated in §5.3.
- Among many possible equilibria predicted by the group-theoretic bifurcation theory, a spatial period-doubling cascade is advanced as the most likely course en route to concentration in one city in §5.4.
- A systematic procedure to obtain equilibrium paths of the core–periphery model is presented in §5.5.

5.1 Symmetry of racetrack economy and governing equation

We consider the racetrack economy with n cities that are equally spread around the circumference of a circle as shown in Fig. 2, and describe the symmetry of these cities and of the governing equation.

Assumption 3 (Parity). We set n to be even as the number of cities treated in the numerical analysis is $n = 4$, 6, 8, and 16 (cf. §6).

[18] The trivial solutions denote solutions for which the population $\boldsymbol{\lambda}$ of the cities remains unchanged in association with the change of the transport parameter τ (cf. Appendix B.2).

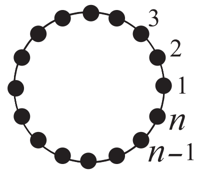

Figure 2: Racetrack among n cities ($n = 16$)

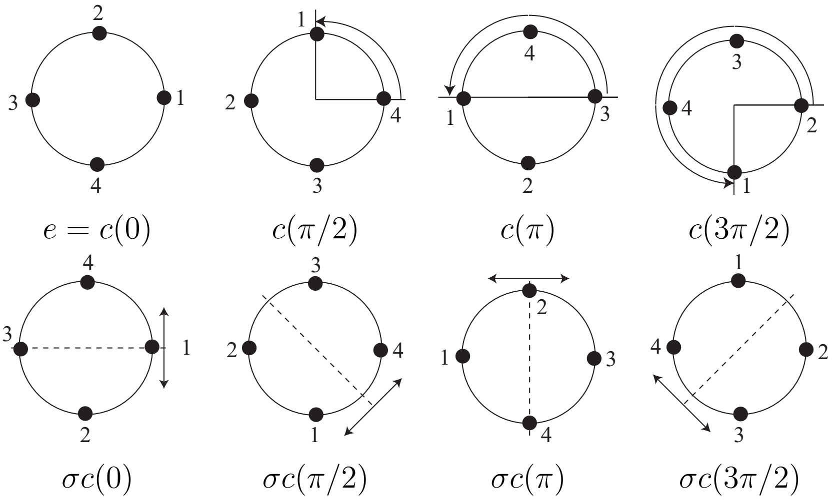

Figure 3: Actions of elements of D_4

5.1.1 Groups for expressing symmetries

The symmetry of these cities can be described as the invariance under geometrical transformations by the dihedral group $G = \mathrm{D}_n$ of degree n expressing regular n-gonal symmetry. This group is defined as

$$\mathrm{D}_n = \{c(2\pi i/n), \sigma c(2\pi i/n) \mid i = 0, 1, \ldots, n-1\},$$

where $\{\cdot\}$ denotes a group consisting of the geometrical transformations in the parentheses, $c(2\pi i/n)$ denotes a counterclockwise rotation about the center of the circle at an angle of $2\pi i/n$ ($i = 0, 1, \ldots, n-1$), and $\sigma c(2\pi i/n)$ is the combined action of the rotation $c(2\pi i/n)$ followed by the upside-down reflection σ (cf. Fig. 3 for $n = 4$).

Bifurcated solutions from the D_n-symmetric racetrack economy have re-

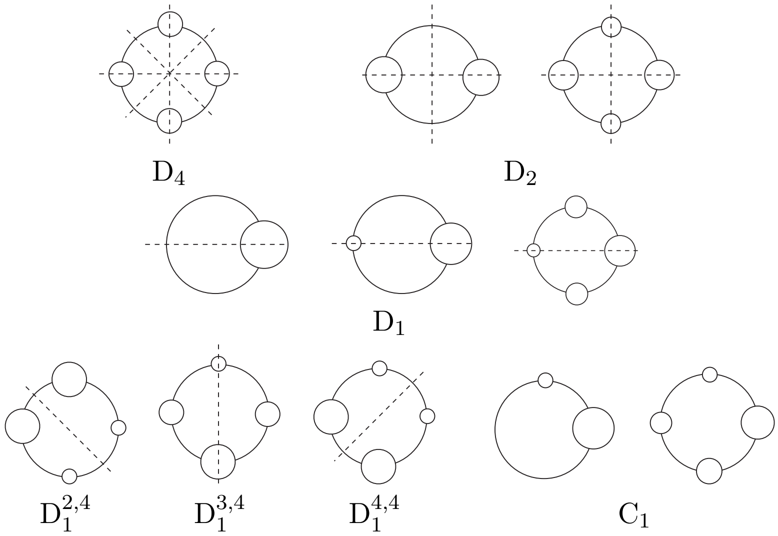

Figure 4: Symmetries of solutions for the four cities ($n = 4$; dashed line, axis of reflection symmetry; the area of ◯ denotes the size of population)

duced symmetries that are labeled by subgroups[19] of D_n. These subgroups are dihedral and cyclic groups that are given respectively as

$$\begin{aligned}\mathrm{D}_m^{k,n} &= \{c(2\pi i/m), \sigma c(2\pi[(k-1)/n + i/m]) \mid i = 0, 1, \ldots, m-1\},\\ \mathrm{C}_m &= \{c(2\pi i/m) \mid i = 0, 1, \ldots, m-1\}.\end{aligned}$$

Therein, the subscript m $(= 1, \ldots, n/2)$ is an integer that divides n; the superscript k $(= 1, \ldots, n/m)$ expresses the directions of the reflection axes. C_m denotes cyclic symmetry at an angle of $2\pi/m$; $\mathrm{D}_m^{k,n}$ denotes reflection symmetry with respect to m-axes together with this cyclic symmetry.

In general, spatial distribution of populations with a higher symmetry with a larger m represents a more uniform state, while that with a lower symmetry with a smaller m represents a more concentrated state.

Example 1 The symmetries of solutions, for example, for the four cities ($n = 4$) are classified by these groups in Fig. 4. The patterns associated with the groups $\mathrm{D}_1^{2,4}$ and $\mathrm{D}_1^{4,4}$ have the same economic meaning; such is also the case for the groups D_1 and $\mathrm{D}_1^{3,4}$. □

[19] $\mathrm{D}_{n/2}^{2,n}$-, C_n-, and $\mathrm{C}_{n/2}$-symmetric modes are absent for this specific racetrack problem.

5.1.2 Spatial periods

In the interpretation of agglomeration patterns, we consider the spatial period T along the unit circle of the racetrack economy. When the cities are invariant under the transformation $c(2\pi i/m)$, i.e., D_m- or $\mathrm{D}_m^{k,n}$-invariant, we define the spatial period as

$$T = T_m = 2\pi/m.$$

Likewise we define the spatial period for the D_n-invariant cities as

$$T = T_n = 2\pi/n.$$

In general, a higher spatial period with a larger m represents a more distributed spatial distribution of populations, a lower spatial period with a smaller m represents a more concentrated distribution.

5.1.3 Equivariance

In the description of the bifurcation of the racetrack economy, the following lemma for the equivariance of this economy is important as it paves the way for application of the group-theoretic bifurcation theory in §4 for a particular case of $G = \mathrm{D}_n$. The rule of hierarchical bifurcations in (16) for $G = \mathrm{D}_n$ varies according to the value of the integer n (cf. Appendix D.1).

Lemma 1 *The nonlinear equality equation* $\boldsymbol{F}(\boldsymbol{\lambda}, \tau) = \mathbf{0}$ *in (10) of the racetrack economy is endowed with equivariance with respect to* D_n*:*

$$T(g)\boldsymbol{F}(\boldsymbol{\lambda}, \tau) = \boldsymbol{F}(T(g)\boldsymbol{\lambda}, \tau), \quad g \in \mathrm{D}_n. \tag{17}$$

Therein $T(g)$ *simultaneously permutes the order of equations via* $T(g)\boldsymbol{F}$ *and the order of independent variables via* $T(g)\boldsymbol{\lambda}$*.*

Proof. See Appendix C. □

5.2 Determination of trivial solutions

The symmetry of the racetrack economy engenders trivial solutions (cf. Appendix B.2), which satisfy, for any values of τ, the nonlinear equality equation $\boldsymbol{F}(\boldsymbol{\lambda}, \tau) = \boldsymbol{0}$ in (10). It is readily apparent that the racetrack economy has the *uniform-population trivial solution*

$$\boldsymbol{\lambda} = (1/n, \ldots, 1/n)^\top \tag{18}$$

with D_n-symmetry and the spatial period of $T_n = 2\pi/n$.

In addition to the uniform population solution in (18), several trivial solutions exist as expounded in Proposition 2.

Proposition 2 *(Period multiplying trivial solutions). There are n/m trivial solutions with*

$$\lambda_i = \begin{cases} 1/m, & (i = k, k + n/m, \ldots, k + (m-1)n/m), \\ 0, & \textit{otherwise} \end{cases} \tag{19}$$

(m divides n; $k = 1, \ldots, n/m$), which, for example, for $k = 1$ is D_m-symmetric. The spatial period $T_m = 2\pi/m$ of these solutions along the circle becomes (n/m)-times as long as the period $T_n = 2\pi/n$ of the uniform population solution in (18).

Proof. See Appendix C. □

Among the trivial solutions in Proposition 2, we are particularly interested in the following trivial solutions:

- *Period-doubling trivial solutions*

  $$\boldsymbol{\lambda} = (2/n, 0, \ldots, 2/n, 0)^\top \text{ and } (0, 2/n, \ldots, 0, 2/n)^\top \tag{20}$$

  express $\mathrm{D}_{n/2}$-symmetric solutions, for which a concentrating city and an extinguishing city alternate along the circle. The spatial period $T_{n/2} = \pi/n$ of these solutions along the circle is doubled in comparison with the period $T_n = 2\pi/n$ of the uniform population solution in (18). Note that the two solutions in (20) have the same economical meaning.

Table 1: Examples of trivial and non-trivial solutions (dashed line, axis of reflection symmetry)

(a) Two cities ($n = 2$)

	D_2	D_1
Trivial	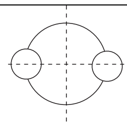	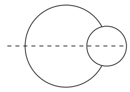
Non-trivial		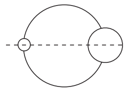

(b) Four cities ($n = 2$)

	D_4	D_2	D_1	$D_1^{2,4}$	C_1
Trivial	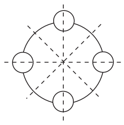	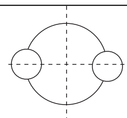	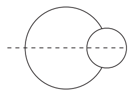	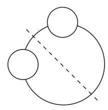	Non-existent
Non-trivial	Non-existent	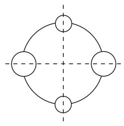	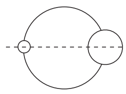	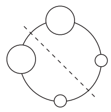	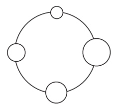

- *Concentrated trivial solutions*

$$\boldsymbol{\lambda} = \big(0, \dots, 0, \overset{i}{1}, 0, \dots, 0\big)^\top, \quad (i = 1, \dots, n)$$

 express the concentration of the population to a single city. The solution for $i = 1$, for example, is D_1-symmetric.

The variety of trivial solutions becomes diverse as the number n of cities increases; see examples below.

Example 2 Two cities ($n = 2$) have only two trivial solutions[20] as shown in Table 1(a):

[20]These trivial solutions were observed by Krugman (1991) [18].

- the uniform population solution $\boldsymbol{\lambda} = (1/2, 1/2)^\top$ (D_2-symmetry), and
- the two concentrated solution $\boldsymbol{\lambda} = (1, 0)^\top$ and $\boldsymbol{\lambda} = (0, 1)^\top$ (D_1-symmetry), which are also the period-doubling trivial solutions.

Example 3 Four cities ($n = 4$) have more trivial solutions (cf. Table 1(b)), such as

- the uniform population solution $\boldsymbol{\lambda} = (1/4, 1/4, 1/4, 1/4)^\top$ (D_4-symmetry),
- the period-doubling trivial solution $\boldsymbol{\lambda} = (1/2, 0, 1/2, 0)^\top$ (D_2-symmetry),
- the concentrated trivial solution $\boldsymbol{\lambda} = (1, 0, 0, 0)^\top$ (D_1-symmetry), and
- $\mathrm{D}_1^{2,4}$-symmetric trivial solution $\boldsymbol{\lambda} = (0, 1/2, 1/2, 0)^\top$, and so on. □

5.3 Bifurcation from the uniform population solution

Bifurcation from the D_n-symmetric uniform population solution in (18) is investigated. Recall that n is assumed to be even.

According to the symmetry conditions (14), the Jacobian matrix J is a symmetric circulant matrix with entries

$$J_{ij} = k_l, \quad (l = \min\{|i-j|,\ n - |i-j|\})$$

for some k_l ($l = 1, 2, \ldots$).

The transformation matrix H for block-diagonalization in (15) is obtainable using the formula in Murota and Ikeda (1991) [22] as

$$H = \begin{cases} (\boldsymbol{\eta}^{(+)}, \boldsymbol{\eta}^{(-)}), & \text{for } n = 2, \\ (\boldsymbol{\eta}^{(+)}, \boldsymbol{\eta}^{(-)}, \boldsymbol{\eta}^{(1),1}, \boldsymbol{\eta}^{(1),2}, \ldots, \boldsymbol{\eta}^{(n/2-1),1}, \boldsymbol{\eta}^{(n/2-1),2}), & \text{for } n \geq 4. \end{cases} \tag{21}$$

The column vectors of this matrix H, which will turn out to be the eigenvectors of J, are expressed as the discrete Fourier series

$$\boldsymbol{\eta}^{(+)} = \frac{1}{\sqrt{n}} \begin{pmatrix} 1 \\ \vdots \\ 1 \end{pmatrix}, \quad \boldsymbol{\eta}^{(-)} = \frac{1}{\sqrt{n}} \begin{pmatrix} \cos \pi \cdot 0 \\ \vdots \\ \cos(\pi(n-1)) \end{pmatrix} = \frac{1}{\sqrt{n}} \begin{pmatrix} 1 \\ -1 \\ \vdots \\ 1 \\ -1 \end{pmatrix}, \tag{22}$$

$$\boldsymbol{\eta}^{(j),1} = \sqrt{\frac{2}{n}} \begin{pmatrix} \cos(2\pi j \cdot 0/n) \\ \vdots \\ \cos(2\pi j(n-1)/n) \end{pmatrix}, \quad \boldsymbol{\eta}^{(j),2} = \sqrt{\frac{2}{n}} \begin{pmatrix} \sin(2\pi j \cdot 0/n) \\ \vdots \\ \sin(2\pi j(n-1)/n) \end{pmatrix},$$
$$(j = 1, \dots, n/2-1). \tag{23}$$

These eigenvectors $\boldsymbol{\eta}^{(+)}$, $\boldsymbol{\eta}^{(-)}$, $\boldsymbol{\eta}^{(j),1}$, and $\boldsymbol{\eta}^{(j),2}$ are D_n-, $\mathrm{D}_{n/2}$-, $\mathrm{D}^{1,n}_{n/\widehat{n}}$-, and $\mathrm{D}^{1+\widehat{n}/2,n}_{n/\widehat{n}}$-symmetric, respectively, and have the spatial periods of $T_n = 2\pi/n$, $T_{n/2} = \pi/n$, $T_{n/\widehat{n}} = \widehat{n}\pi/n$, and $T_{n/\widehat{n}} = \widehat{n}\pi/n$, respectively. Here

$$\widehat{n} = n/\mathrm{gcd}\,(j, n) \geq 3, \tag{24}$$

and $\mathrm{gcd}\,(j, n)$ is the greatest common divisor of j and n.

The block-diagonal form in (15) reduces to a diagonal matrix as

$$\tilde{J} = H^\top J H = \mathrm{diag}(e^{(+)},\ e^{(-)},\ e^{(1)},\ e^{(1)},\ \dots,\ e^{(n/2-1)},\ e^{(n/2-1)}),$$

where $\mathrm{diag}(\cdot)$ denotes a diagonal matrix with the diagonal entries therein. The diagonal entries, which correspond to the eigenvalues of J, are

$$e^{(+)} = k_0 + k_{n/2} + 2\sum_{l=1}^{n/2-1} k_l, \tag{25}$$

$$e^{(-)} = k_0 + (-1)^{n/2} k_{n/2} + 2\sum_{l=1}^{n/2-1} (-1)^l k_l, \tag{26}$$

$$e^{(j)} = k_0 + \cos(\pi j)\ k_{n/2} + 2\sum_{l=1}^{n/2-1} \cos(2\pi j l/n)\ k_l, \quad (j = 1, \dots, n/2-1). \tag{27}$$

It is noteworthy that $e^{(+)}$ and $e^{(-)}$ are simple eigenvalues, and that $e^{(j)}$ $(j = 1, \dots, n/2-1)$ are double eigenvalues that are repeated twice.

We can classify critical points on the uniform population solution as

$$\begin{cases} e^{(+)} = 0: & \text{limit point of } \tau\ (M = 1), \\ e^{(-)} = 0: & \text{simple bifurcation point } (M = 1), \\ e^{(j)} = 0: & \text{double bifurcation point } (M = 2). \end{cases}$$

These simple and double bifurcation points are break bifurcation points.

The simple bifurcation point with $e^{(-)} = 0$ corresponds to the spatial period-doubling bifurcation, which engenders an alternating equilibrium (cf. Proposition 3).

Proposition 3 *(Simple bifurcation). At the simple bifurcation point, which is either a pitchfork or tomahawk, we encounter a symmetry-breaking bifurcation* $\mathrm{D}_n \longrightarrow \mathrm{D}_{n/2}$. *Its critical eigenvector is given uniquely as a* $\mathrm{D}_{n/2}$*-symmetric vector* $\boldsymbol{\eta}^{(-)}$ *of (22) with components of alternating signs expressing the bifurcation mode of spatial period doubling from* $T = 2\pi/n$ *to* π/n.

The double bifurcation point $e^{(j)} = 0$ for some j corresponds to the spatial period $\widehat{n}$-times bifurcation (cf. (24) for the definition of $\widehat{n}$), which engenders a more rapid concentration than the period doubling bifurcation of the simple bifurcation point (cf. Proposition 4). Double bifurcation points with $e^{(j)} = 0$ are absent for the two cities with $n = 2$ (cf. (21)). It exercises caution that the bifurcation of the two cities is a special case, while four or more cities in general have double bifurcation points and have different bifurcation properties.

Proposition 4 *(Double bifurcation). At the double bifurcation point with* $e^{(j)} = 0$ *for some* j*, we encounter a symmetry-breaking bifurcation* $\mathrm{D}_n \longrightarrow \mathrm{D}_{n/\widehat{n}}$*, at which the spatial period becomes* $\widehat{n}$*-times (*$\widehat{n} \geq 3$ *by (24)).*

Proof. See Appendix C. □

Example 4 The change of symmetry at bifurcation points is illustrated in Fig. 5 for the four cities ($n = 4$). At the simple bifurcation point in Fig. 5(a), the bifurcation doubles the spatial period and triggers concentration of the population to two cities located at opposite sides of the circle, while the populations of the other two cities decline. At the double bifurcation point in Fig. 5(b) associated with $e^{(j)} = 0$ ($n = 4$, $j = 1$, $\widehat{n} = 4$), the spatial period becomes four times. □

5.4 Spatial period-doubling cascade

In addition to break bifurcations from the uniform-population trivial solution with D_n-symmetry that were studied in §5.3, several possible sources of symmetry-breaking exist. Namely, further break bifurcations may be encountered on (a) bifurcated paths of this D_n-symmetric solution and (b) D_m-symmetric trivial solutions (m divides n) presented in §5.2.

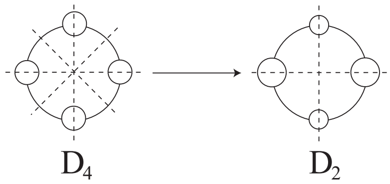

(a) Simple bifurcation

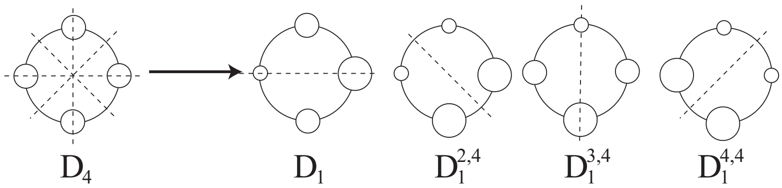

(b) Double bifurcation

Figure 5: Direct bifurcations from the four uniform cities ($n = 4$; the arrow denotes the occurrence of a bifurcation)

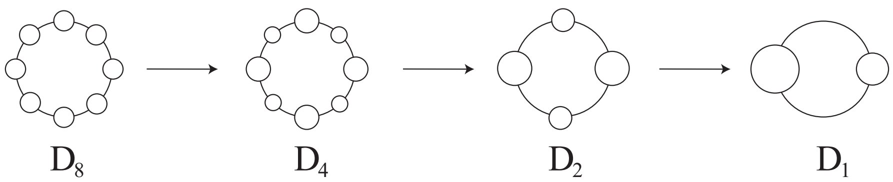

Figure 6: Spatial period-doubling cascade for the eight cities ($n = 8$; the arrow denotes the occurrence of a bifurcation)

All these break bifurcations can be described by group-theoretic bifurcation theory (cf. Ikeda and Murota, 2002 [16]). The rule of bifurcation depends on the integer number n, to be precise, the divisors of the number n. The bifurcation becomes increasingly hierarchical and complex for n with more divisors (cf. Appendix D).

Among possible courses of hierarchical bifurcations, we pay special attention to the *spatial period-doubling bifurcation* for D_n-symmetric cities with $n = 2^k$ (k is some positive integer) that is expounded in Proposition 5 below. Figure 6 depicts this bifurcation for $n = 8 = 2^3$ cities.

Proposition 5 *(Spatial period-doubling cascade).* D_n*-symmetric cities with*

$n = 2^k$ for some integer k have a possible course:

$$\mathrm{D}_{2^k} \longrightarrow \mathrm{D}_{2^{k-1}} \longrightarrow \mathrm{D}_{2^{k-2}} \longrightarrow \cdots \longrightarrow \mathrm{D}_1 \tag{28}$$

that is called "spatial period-doubling cascade[21]," in which the spatial period is doubled successively by repeated simple bifurcations.

Remark 2 Proposition 5 serves as a generalization of the study of Tabuchi and Thisse (2009) [27] who conducted a local analysis (linearized eigenproblem) for the flat distribution of the racetrack economy to predict of the occurrence of the period doubling cascade. In comparison with the study by Tabuchi and Thisse (2009) [27], the implementation of the income effect for good consumption of the core–periphery model, i.e., an increase in goods consumption in association with an increase in the income, is a possible improvement of this paper from an economics standpoint.

5.5 Systematic procedure to obtain equilibrium paths

We present a systematic procedure to obtain equilibrium paths of the core–periphery model. First, we conduct the exhaustive search by obtaining all the equilibrium paths using the following steps:

Step 1: Obtain all trivial solutions by the method presented in §5.2.

Step 2: Carry out the eigenanalysis of the Jacobian matrix J, on these trivial solutions to obtain the bifurcation points and to classify feasible and infeasible solutions. On the uniform population solution, the formulas (25)–(27), which give the eigenvalues analytically, are to be employed, while the numerical eigenanalysis is to be conducted for other trivial solutions.

Step 3: Obtain the bifurcated paths branching from all these trivial solutions by the computational bifurcation theory in Appendix E. The numerical

[21] A repeated doubling of time period by bifurcations takes place in many physical systems (Feigenbaum, 1978 [8]) and is called period doubling cascade.

eigenanalysis is to be conducted to find critical points and testify the feasibility of these solutions.

Step 4: Repeat the Steps 3 and 4 to exhaust all equilibrium paths.

Next, among all these equilibrium paths we select feasible ones that are to be encountered when the transport cost τ is decreased from ∞ to 0. Existence and multiplicity of possible feasible ones for a particular value of τ depend on the umber n of cities, the values of the parameters σ and μ, and so on, and must be investigated individually.

6 Bifurcation analysis of racetrack economy

Agglomerations of the racetrack economy are investigated for $n = 4$, 6, 8, and 16 cities. The solutions of a system of governing equations (10) and (11) of the core–periphery model are obtained by the systematic procedure to obtain equilibrium paths in §5.5. The progress of agglomeration is expressed as successive breaking of symmetries associated with successive elongation of the spatial period with reference to the theoretical rule of bifurcation presented in §5. Successive and gradual progress of agglomerations by the spatial period-doubling cascade in Proposition 5 is highlighted as a key phenomenon for $n = 4$, 8, and 16 cities in §6.1. The period-doubling and period-tripling are observed for $n = 6$ cities in §6.2.

We set the elasticity of substitution as $\sigma = 10.0$ and the ratio of the manufacturing labor force as $\mu = 0.4$. The transport parameter τ, which is proportional to the transport cost t_{ij} via (7) and stays in the range $[0, \infty]$, is scaled as

$$\tau' = 1 - \exp(-\tau\pi); \tag{29}$$

$\tau' = 0$ ($\tau = 0$) corresponds to the state of no transport cost, and $\tau' = 1$ ($\tau = +\infty$) corresponds to the state of infinite transport cost.

6.1 Period Doubling Cascade

We demonstrate the occurrence of period doubling cascade for $n = 4$, 8, and 16 cities.

6.1.1 Four cities

For the four cities ($n = 4$), equilibrium paths were obtained by the by the systematic procedure to obtain equilibrium paths in §5.5. Figure 7(a) shows τ' versus λ_1 curves obtained in this manner, where the ordinate $\tau' = 1 - \exp(-\tau\pi)$ is a scaled transport parameter in (29). Economically feasible solutions (shown as solid curves) and infeasible ones (as dotted curves) are classified using Proposition 1 in §3.2. Trivial paths (solutions) with D_m-symmetries ($m = 1, 2, 4$) exist at the horizontal lines at $\lambda_1 = 0$, $1/4$, $1/2$,

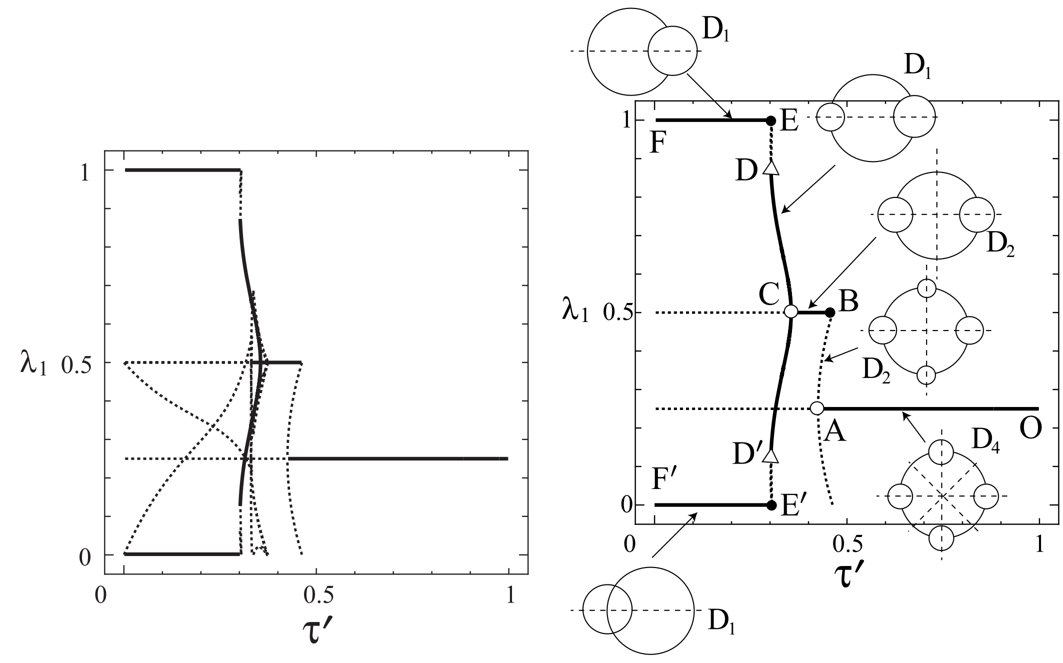

(a) All equilibrium paths

(b) Feasible trivial paths and associated paths

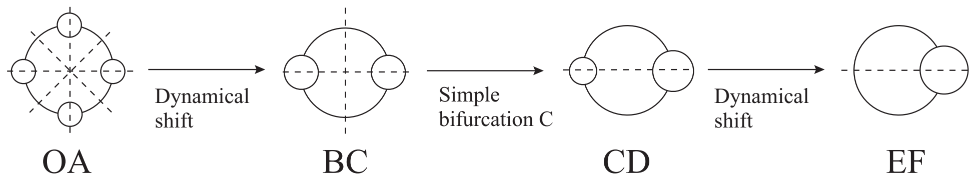

(c) Predicted shift of feasible solutions as τ' decreases

Figure 7: Equilibrium paths of the four cities ($n = 4$) and a predicted shift of feasible solutions in association with the decrease of transport cost ($\tau' = 1 - \exp(-\tau\pi)$; solid curve, feasible; dashed curve, infeasible; $\circ$, simple break point; $\triangle$, limit point; $\bullet$, sustain point)

and 1 (cf. Table 1(b) in §5.2), and several bifurcated paths connecting these trivial paths exist. These paths are apparently quite complex.

To assist the economical interpretation, among such complex paths, we have chosen feasible trivial paths and associated paths shown in Fig. 7(b) as those most likely to occur; distributions of populations are portrayed at several equilibrium points. Economically feasible parts (shown as solid lines) of the trivial solutions are

- OA: uniform population solution $\boldsymbol{\lambda} = (1/4, 1/4, 1/4, 1/4)^\top$ (D_4-symmetry),
- BC: period-doubling solution $\boldsymbol{\lambda} = (1/2, 0, 1/2, 0)^\top$ (D_2-symmetry),
- EF: concentrated solution $\boldsymbol{\lambda} = (1, 0, 0, 0)^\top$ (D_1-symmetry), and
- E′F′: another concentrated solution $\boldsymbol{\lambda} = (0, 0, 1, 0)^\top$ (D_1-symmetry).

Note that EF and E′F′ are symmetric counterparts with the same economical meaning.

Bifurcation points on these trivial solutions are classifiable as break and sustain points (cf. Appendix B.4). Symmetries of the system are reduced at period-doubling breaking bifurcation points A and C denoted as $\circ$ (cf. Appendix D.1):

- At A, we encounter a symmetry breaking $D_4 \longrightarrow D_2$ associated with
$$\boldsymbol{\lambda} = (1/4, 1/4, 1/4, 1/4)^\top \to (1/4 + \alpha, 1/4 - \alpha, 1/4 + \alpha, 1/4 - \alpha)^\top,$$
($|\alpha| < 1/4$).
- At C, we encounter a symmetry breaking $D_2 \longrightarrow D_1$ associated with
$$\boldsymbol{\lambda} = (1/2, 0, 1/2, 0)^\top \to (1/2 + \alpha, 0, 1/2 - \alpha, 0)^\top, \quad (|\alpha| < 1/2).$$

Symmetries are preserved at the sustain points denoted as $\bullet$, at which a trivial solution and a non-trivial one intersect (Appendix D). Sustain point B has D_2-symmetry; E and E′, D_1-symmetry.

Among the bifurcated paths, we found the path CD and its symmetric counterpart CD′ feasible. The feasible path CD became infeasible at the limit (maximum) point τ at D denoted by $\triangle$ (cf. the left of Fig. 11(a) in Appendix B.3).

In view of the whole set of feasible paths obtained herein, in association with the decrease of τ', we predict a possible course of the accumulation of population following four feasible stages: OA, BC, CD, and EF, as presented in Fig. 7(c). Dynamical shifts are assumed between OA and BC and between CD and EF. Starting from the uniform state $\boldsymbol{\lambda} = (1/4, 1/4, 1/4, 1/4)^\top$, via bifurcations and dynamical shifts, we arrive at the complete concentration $\boldsymbol{\lambda} = (1, 0, 0, 0)^\top$, in agreement with the rule of bifurcations in Fig. 13(a) in Appendix D.1. We can see the occurrence of a spatial period-doubling cascade

$$\mathrm{D}_4 \longrightarrow \mathrm{D}_2 \longrightarrow \mathrm{D}_1,$$

en route to the concentration to a single city, in agreement with Proposition 5 in §5.4.

Recall that the feasible solutions of the simple tomahawk bifurcation[22] of the two cities consisted only of two trivial solutions: the uniform population solution and the completely concentrated solution (cf. Table 1(a)). Different from the two cities, the four cities have a feasible non-trivial solution[23] CD, for which migration from one city to another occurs in an economically feasible manner without undergoing bifurcation. Moreover, the progress of agglomeration of the four cities is much more complex than that of the spontaneous concentration of the two cities triggered by the simple tomahawk bifurcation. It demands caution that the experience of the two cities is not universal, thereby underscoring the importance of bifurcation analysis for many cities examined in the remainder of this section.

6.1.2 Eight cities

For the eight cities bifurcated paths branching from several trivial solutions are obtained in an exhaustive manner as shown in τ' versus λ_1 relationship

[22] The tomahawk bifurcation was observed, e.g., in Krugman (1991) [18] and Fujita et al. (1999) [10] for the present model, and in Forslid and Ottaviano (2003) [9] for an analytically solvable model.

[23] A feasible non-trivial solution was observed also by Pflüger (2004) [25] for a simple, analytically-solvable model for the two cities.

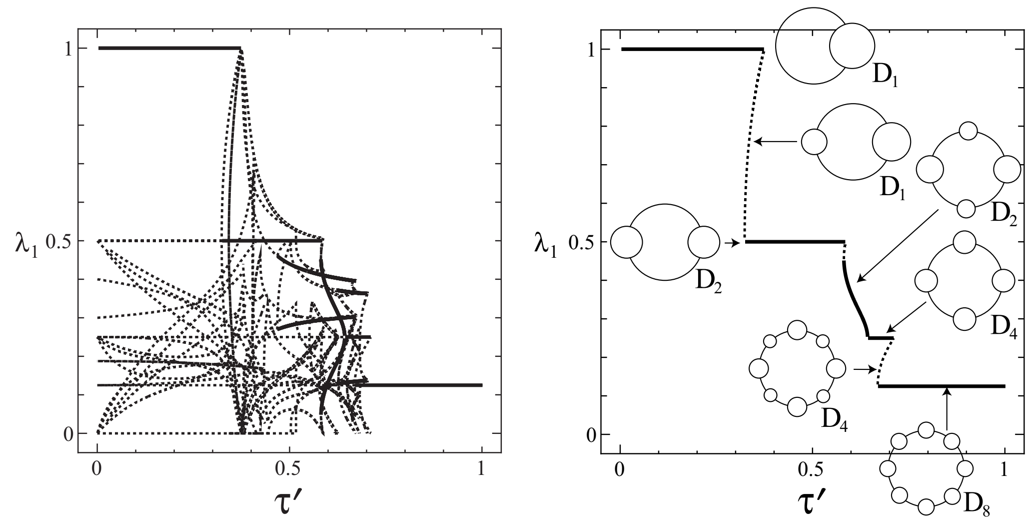

(a) All equilibrium paths

(b) Feasible trivial paths and associated paths

Figure 8: Equilibrium paths of the eight cities expressed in terms of τ' versus λ_1 curves ($n = 8$; $\tau' = 1 - \exp(-\tau\pi)$; solid curve, feasible; dashed curve, infeasible)

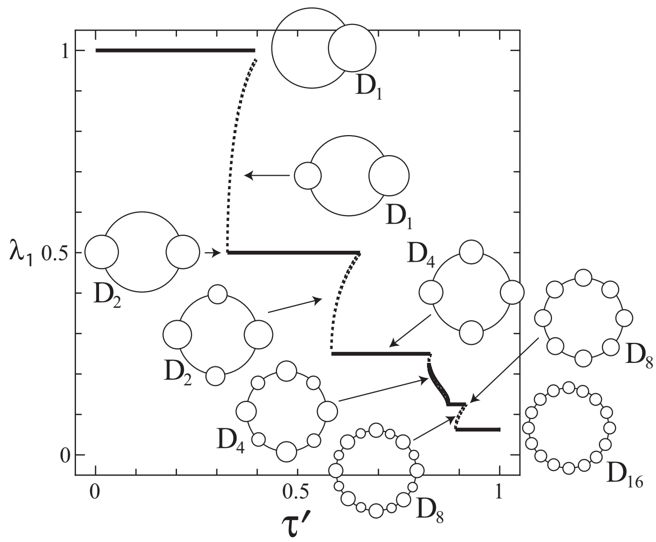

Figure 9: Feasible trivial paths and associated paths for the 16 cities that are expected to be followed in association with a decrease of τ' ($n = 16$; $\tau' = 1 - \exp(-\tau\pi)$; solid curve, feasible; dashed curve, infeasible)

of Fig. 8(a). The horizontal lines at $\lambda_1 = 0$, $1/8$, $1/4$, $1/2$, and 1 are trivial solutions with D_m-symmetries ($m = 1, 2, 4, 8$); these bifurcated paths that connect these trivial solutions have grown more complex than those for the six cities in Fig. 10(a).

Among all the equilibrium paths for the eight cities shown in Fig. 8(a), feasible equilibrium paths that are expected to be followed in association with the decrease of τ' are depicted in Fig. 8(b). The spatial period-doubling cascade

$$\mathrm{D}_8 \longrightarrow \mathrm{D}_4 \longrightarrow \mathrm{D}_2 \longrightarrow \mathrm{D}_1 \tag{30}$$

engenders concentration into four cities and then into two cities, en route to concentration to a single city.

Complex bifurcated paths connecting these trivial solutions were found in Fig. 8(a). Such complexity, notwithstanding, all these paths have been traced successfully by the systematic procedure to obtain equilibrium paths in §5.5; it demonstrates the prowess of this procedure. In addition, the rule of break bifurcations in Fig. 13(b) in Appendix D.1 was of assistance in the tracing of bifurcated paths. One might feel pessimistic when observing the complexity of the bifurcation of the racetrack economy that will grow rapidly with the increase of the number n of cities. Nonetheless, we can resolve such pessimism by addressing only feasible solutions, as in the spatial period-doubling cascade (30).

6.1.3 16 cities

Similarly to the four and eight cities, the 16 cities displayed the spatial-period doubling cascade, as shown in Fig. 9,

$$\mathrm{D}_{16} \longrightarrow \mathrm{D}_8 \longrightarrow \mathrm{D}_4 \longrightarrow \mathrm{D}_2 \longrightarrow \mathrm{D}_1.$$

6.1.4 Discussion

The presence of spatial-period doubling cascade, which was predicted in Tabuchi and Thisse (2009) [27] and also by group-theoretic bifurcation theory in Proposition 5, has thus been ensured. It is highlighted as a mechanism to engender concentration out of uniformity, especially for $n = 2^k$ cities. It is to be remarked again that, unlike the two-city special case, there are feasible non-trivial solutions.

6.2 Period doubling and tripling: six cities

Equilibrium paths of the six cities are shown in Fig. 10(a), from which we chose feasible paths and some associated paths shown in Fig. 10(b).

There are trivial solutions with D_m-symmetries ($m = 1, 2, 3, 6$) (cf. §5.2) at the horizontal lines at $\lambda_1 = 0$, $1/6$, $1/3$, $1/4$, $1/2$, and 1:

- $\lambda_1 = 1/6$: D_6-symmetric uniform population solution,
- $\lambda_1 = 0$, $1/3$: D_3-symmetric period-doubling trivial solutions,
- $\lambda_1 = 0$, $1/4$, $1/2$: D_2-symmetric trivial solutions, and
- $\lambda_1 = 0$, 1: D_1-symmetric concentrated trivial solutions.

We observed

- period doubling simple break bifurcations: $\mathrm{D}_6 \longrightarrow \mathrm{D}_3$ and $\mathrm{D}_2 \longrightarrow \mathrm{D}_1$;
- period tripling double break bifurcations: $\mathrm{D}_6 \longrightarrow \mathrm{D}_2$ and $\mathrm{D}_3 \longrightarrow \mathrm{D}_1^{k,6}$.

This is due to the fact that $n = 6$ has two divisors: 2 and 3. Thus the period doubling is not that dominant as the four cities (cf. Fig. 7(b)), while the period tripling via double break bifurcations plays an important role. The period tripling, which is theoretically predicted in Proposition 2 with $\widehat{n} = 3$, does not take place for $n = 2^k$ cities, including the two cities.

A predicted shift of feasible solutions occurring in association with the decrease of τ' is presented in Fig. 10(c). This shift is not unique:

- The D_6-symmetric state might dynamically jump into either the D_2- or D_3-symmetric state.
- The D_3-symmetric state might dynamically jump into the D_2- or $\mathrm{D}_1^{5,6}$-symmetric state.

By virtue of the mixed occurrence of the period doubling and tripling, the predicted shift for the six cities with $n = 6 = 2 \times 3$ is more complex than that of the four cities portrayed in Fig. 7(b).

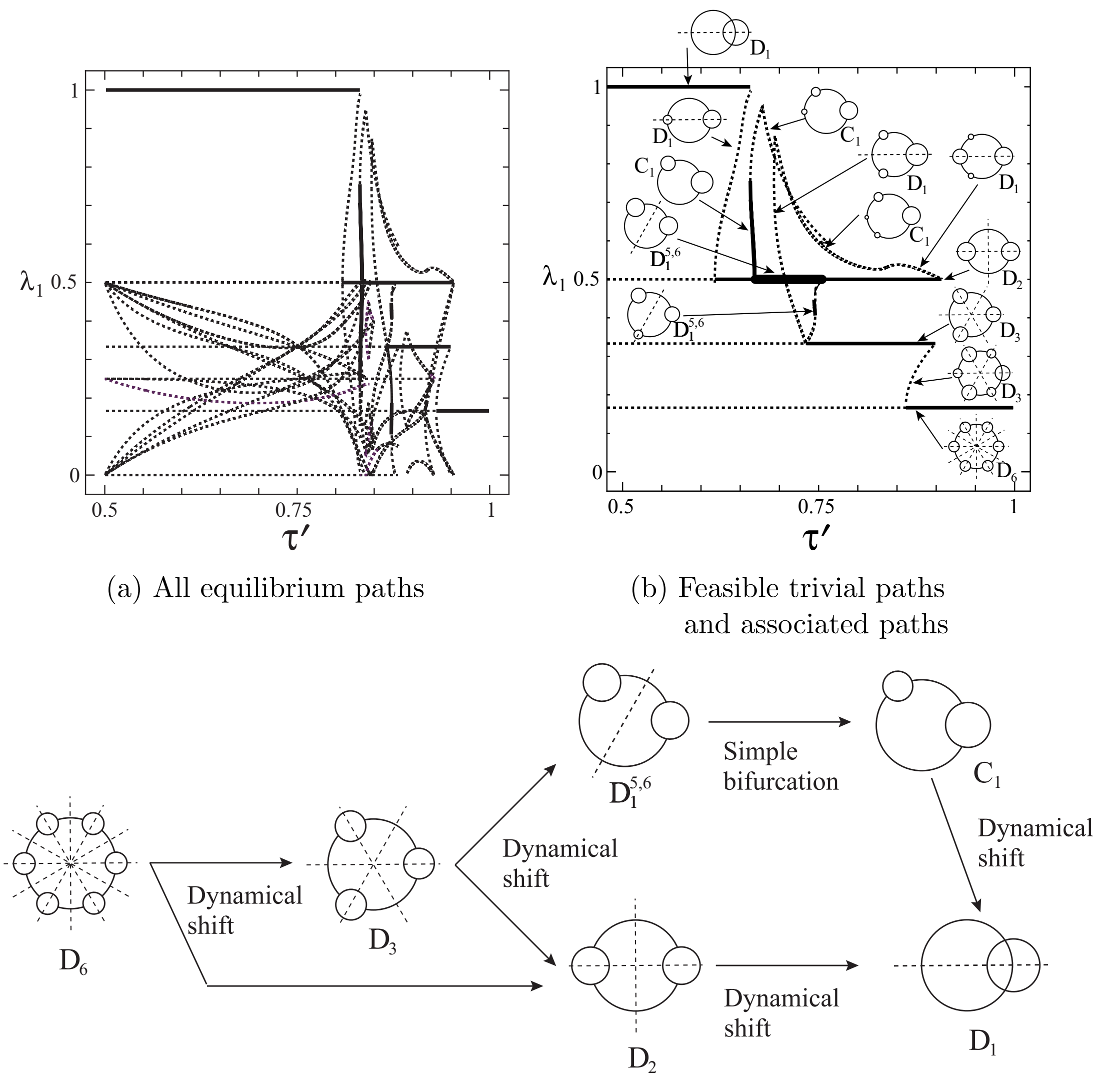

(a) All equilibrium paths

(b) Feasible trivial paths and associated paths

(c) Predicted shift of feasible solutions as τ' decreases

Figure 10: Equilibrium paths of the six cities ($n = 6$; $\tau' = 1 - \exp(-\tau\pi)$; solid curve, feasible; dashed curve, infeasible)

7 Conclusions

To testify the adequacy of the two-city special case as a platform for spatial agglomerations, we investigated the progress of agglomerations of the racetrack economy of the core–periphery model with four, six, eight, and 16 cities. These cities displayed several features, including:

- feasible non-trivial solutions,
- period-doubling cascade,
- a plethora of bifurcated paths, and
- period tripling via double break bifurcations.

These features were not observed and can be overlooked in Kruhgman's two-city special case, in which the tomahawk bifurcation engenders spontaneous concentration to a single city. It demands caution that the experience of the two-city special case with a simple tomahawk bifurcation is not universal. It is preferable to employ a system of cities as a platform for the investigation of spatial agglomerations.

Symmetry-breaking bifurcation predicted by group-theoretic bifurcation theory proposed a broader view on the bifurcation of the racetrack economy. In fact, the bifurcation phenomena become progressively complex in association with the increase of the number of cities. Such complexity might instill pessimism about the usefulness of the bifurcation analysis of the racetrack economy. Yet, when we specifically examine economically feasible solutions that are expected to occur in association with the decrease of the transport cost, the spatial period-doubling cascade can be highlighted as the most likely mechanism to engender concentration out of uniformly distributed population. This suffices to clarify the pessimism.

Such complex phenomena can be traced in an exhaustive and systematic manner owing to the insight of group-theoretic bifurcation theory. The proposed procedure is applicable to any new economic geography models other than Krugman's core–periphery model, and also to city distributions other than the racetrack economy. Accordingly, it will be a topic of future studies to carry out bifurcation analysis of other updated new economic geography models with a system of cities scattered on a two-dimensional domain.

References

[1] Baldwin, R., Forslid, R, Martin, P., Ottaviano G., Robert-Nicoud, F., 2003. *Economic Geography and Public Policy.* Princeton University Press.

[2] Behrens, K., Thisse, J.-F., 2007. Regional economics: A new economic geography perspective. *Regional Science and Urban Economics* 37(4) 457–465.

[3] Brakman, S., Garretsen, H., van Marrewijk, C., 2001. *The New Introduction to Geographical Economics.* Cambridge University Press.

[4] Combes, P. P., Mayer, T., Thisse, J. F., 2008. *Economic Geography: The Integration of Regions and Nations.* Princeton University Press.

[5] Crisfield, M. A., 1977. *Non-linear Finite Element Analysis of Solids and Structures.* Wiley.

[6] Dixit, A., Stiglitz, J., 1977. Monopolistic competition and optimum product diversity, *American Economic Review* 67, 297-308.

[7] Facchinei, F., Pang, J.-S., 2003. *Finite-Dimensional Variational Inequalities and Complementarity Problems*, Vol.I & II. Springer-Verlag.

[8] Feigenbaum, M. J., 1978. Qualitative universality for a class of nonlinear transformations. *Journal of Statistical Physics* 19 25–52.

[9] Forslid, R., Ottaviano, G. I. P., 2003. An analytically solvable core–periphery model, *Journal of Economic Geography* 3 229–240.

[10] Fujita, M., Krugman, P., Venables, A. J., 1999. *The Spatial Economy.* MIT Press.

[11] Fujita, M., Thisse, J. F., 2002. *Economics of Agglomeration*. Cambridge University Press.

[12] Fujita, M., Thisse, J. F., 2009. New economic geography: an appraisal on the occasion of Paul Krugman's 2008 nobel prize in economic sciences. *Regional Science and Urban Economics* 39(2), 109-250.

[13] Glaeser, E. L., 2008. *Cities, Agglomeration and Spatial Equilibrium*. Oxford University Press.

[14] Golubitsky, M., Stewart, I., Schaeffer, D. G., 1988. *Singularities and Groups in Bifurcation Theory*, Vol.II. Springer-Verlag.

[15] Henderson, J. V. Thisse, J. F. eds., 2004. *Handbook of Regional and Urban Economics 4, Cities and Geography*. Elsevier.

[16] Ikeda, K., Murota, K., 2002. *Imperfect Bifurcation in Structures and Materials*. Springer-Verlag.

[17] Ikeda, K., Murota, K., Fujii, H., 1991. Bifurcation hierarchy of symmetric structures. *International Journal of Solids and Structures* 27(12) 1551–1573.

[18] Krugman, P., 1991. Increasing returns and economic geography. *Journal of Political Economy* 99 483–499.

[19] Krugman, P., 1993. On the number and location of cities. *European Economic Review* 37 293–298.

[20] Krugman, P., 1996. *The Self-Organizing Economy*. Blackwell.

[21] Lorenz, H. W., 1997. *Nonlinear Dynamical Economics and Chaotic Motion*. Springer-Verlag.

[22] Murota, K., Ikeda, K., 1991. Computational use of group theory in bifurcation analysis of symmetric structures. *SIAM Journal of Scientific and Statistical Computing* 12(2) 273–297.

[23] Nagurney, A., 1993. *Network Economics*. Kluwer.

[24] Ottaviano, G. I. P., Puga, D., 1998. Agglomeration in the Global Economy: A Survey of the 'New Economic Geography.' *The World Economy* 21(6) 707–731.

[25] Pflüger, M., 2004. A simple, analytically solvable, Chamberlinian agglomeration model. *Regional Science and Urban Economics* 34(5) 565–573.

[26] Picard, P. M. Tabuchi, T., 2009. Self-organized agglomerations and transport costs. *Economic Theory* DOI 10.1007/s00199-008-0410-4.

[27] Tabuchi, T., Thisse, J. F., 2009. Self-organizing urban hierarchy. Preprint.

A Derivation of incremental equation

To derive the incremental equation for the equality (10), we rewrite the complementary condition (5) as

$$\boldsymbol{P}(\boldsymbol{\lambda}, \boldsymbol{w}, \bar{\omega}, \tau) = \begin{pmatrix} (\omega_1(\boldsymbol{w}, \tau) - \bar{\omega})\lambda_1 \\ \vdots \\ (\omega_n(\boldsymbol{w}, \tau) - \bar{\omega})\lambda_n \end{pmatrix} = \boldsymbol{0}, \tag{A.1}$$

$$\omega_i(\boldsymbol{w}, \tau) - \bar{\omega} \leq 0, \quad \lambda_i \geq 0, \quad (i = 1, \ldots, n). \tag{A.2}$$

Here $\boldsymbol{w} = (w_1, \ldots, w_n)^\top$ and $\omega_i = \omega_i(\boldsymbol{w}, \tau)$ $(i = 1, \ldots, n)$ by (4).

Equation (1) is expressed as

$$\boldsymbol{M}(\boldsymbol{\lambda}, \boldsymbol{w}, \tau) = \begin{pmatrix} \big[\sum_{s=1}^{n} Y_s (t_{1s})^{1-\sigma} G_s^{\sigma-1}\big] - \big(w_1\big)^{\sigma} \\ \vdots \\ \big[\sum_{s=1}^{n} Y_s (t_{ns})^{1-\sigma} G_s^{\sigma-1}\big] - \big(w_n\big)^{\sigma} \end{pmatrix} = \boldsymbol{0}, \tag{A.3}$$

and the conservation law (6) is ($\boldsymbol{1} = (1, \ldots, 1)^\top$)

$$F(\boldsymbol{\lambda}) = \boldsymbol{1}^\top \boldsymbol{\lambda} - 1 = 0. \tag{A.4}$$

An assembly of the relations (A.1), (A.3), and (A.4) gives the set of $2n+1$ nonlinear equations

$$\begin{pmatrix} \boldsymbol{P}(\boldsymbol{\lambda}, \boldsymbol{w}, \bar{\omega}, \tau) \\ \boldsymbol{M}(\boldsymbol{\lambda}, \boldsymbol{w}, \tau) \\ F(\boldsymbol{\lambda}) \end{pmatrix} = \boldsymbol{0} \tag{A.5}$$

with a bifurcation parameter τ and $2n + 1$ independent variables $\boldsymbol{\lambda}$, $\boldsymbol{w}$, and $\bar{\omega}$.

We rewrite (A.5) into an incremental form:

$$\frac{\partial \boldsymbol{P}}{\partial \boldsymbol{\lambda}} \delta\boldsymbol{\lambda} + \frac{\partial \boldsymbol{P}}{\partial \boldsymbol{w}} \delta\boldsymbol{w} + \frac{\partial \boldsymbol{P}}{\partial \bar{\omega}} \delta\bar{\omega} + \frac{\partial \boldsymbol{P}}{\partial \tau} \delta\tau = \boldsymbol{0}, \tag{A.6}$$

$$\frac{\partial \boldsymbol{M}}{\partial \boldsymbol{\lambda}} \delta\boldsymbol{\lambda} + \frac{\partial \boldsymbol{M}}{\partial \boldsymbol{w}} \delta\boldsymbol{w} + \frac{\partial \boldsymbol{M}}{\partial \tau} \delta\tau = \boldsymbol{0}, \tag{A.7}$$

$$\frac{\partial F}{\partial \boldsymbol{\lambda}} \delta\boldsymbol{\lambda} = 0 \tag{A.8}$$

(cf. Ikeda and Murota, 2002, Chapter 7 [16]), in which $\partial F/\partial \boldsymbol{\lambda} = \mathbf{1}$ by (A.4). Under Assumption 4, it is possible to eliminate independent variables $\delta \boldsymbol{w}$ and $\delta\bar{\omega}$ from (A.6)∼(A.8) as shown below:

$$\begin{aligned}
\delta \boldsymbol{w} &= \left(\frac{\partial \boldsymbol{M}}{\partial \boldsymbol{w}}\right)^{-1}\left(\frac{\partial \boldsymbol{M}}{\partial \boldsymbol{\lambda}} J^{-1}\frac{\partial \boldsymbol{F}}{\partial \tau} - \frac{\partial \boldsymbol{M}}{\partial \tau}\right)\delta\tau, \\
\delta\bar{\omega} &= -T\delta\tau,
\end{aligned}$$

and, in turn, to arrive at an incremental equilibrium equation

$$\tilde{\boldsymbol{F}}(\delta\boldsymbol{\lambda}, \delta\tau) = J\delta\boldsymbol{\lambda} + \frac{\partial \boldsymbol{F}}{\partial \tau}\delta\tau + \text{h.o.t.} = \mathbf{0}, \tag{A.9}$$

where h.o.t. dentoes higher order terms and

$$\begin{aligned}
J &= \frac{\partial \boldsymbol{F}}{\partial \boldsymbol{\lambda}} = \frac{\partial \boldsymbol{P}}{\partial \boldsymbol{\lambda}} - \frac{\partial \boldsymbol{P}}{\partial \boldsymbol{w}}\left(\frac{\partial \boldsymbol{M}}{\partial \boldsymbol{w}}\right)^{-1}\frac{\partial \boldsymbol{M}}{\partial \boldsymbol{\lambda}}, \\
\frac{\partial \boldsymbol{F}}{\partial \tau} &= \boldsymbol{S} - T\frac{\partial \boldsymbol{P}}{\partial \bar{\omega}}, \\
\boldsymbol{S} &= \frac{\partial \boldsymbol{P}}{\partial \tau} - \frac{\partial \boldsymbol{P}}{\partial \boldsymbol{w}}\left(\frac{\partial \boldsymbol{M}}{\partial \boldsymbol{w}}\right)^{-1}\frac{\partial \boldsymbol{M}}{\partial \tau}, \quad T = \frac{\dfrac{\partial F}{\partial \boldsymbol{\lambda}} J^{-1}\boldsymbol{S}}{\dfrac{\partial F}{\partial \boldsymbol{\lambda}} J^{-1}\dfrac{\partial \boldsymbol{P}}{\partial \bar{\omega}}}.
\end{aligned}$$

Assumption 4 (Regularity conditions.) The incremental governing equation (A.9) was derived under the assumptions that the matrices J and $\partial \boldsymbol{M}/\partial \boldsymbol{w}$ are nonsingular, and that the scalar $\partial F/\partial \boldsymbol{\lambda} J^{-1}\partial \boldsymbol{P}/\partial\bar{\omega}$ is nonzero.

B Classifications and definition of equilibrium points

In the study of the agglomeration of the core–periphery model, it is useful to resort to various kinds of classifications of equilibrium points.

B.1 Interior and corner solutions

Solutions of this model are classifiable into two types:

- an interior solution for which all cities have positive population $\lambda_i > 0$ $(i = 1, \dots, n)$, and
- a corner solution for which some cities have zero population.

The existence of the corner solution is a special feature of the core–periphery model that demands reorganization in the application of bifurcation theory (cf. Appendix D).

B.2 Trivial and non-trivial solutions

The core–periphery model has characteristic solutions, for which the population $\boldsymbol{\lambda}$ of the cities remains unchanged in association with the change of the transport parameter τ. We accordingly have classification:

$$\begin{cases} \text{Trivial solution:} & \boldsymbol{\lambda} \text{ is constant with respect to } \tau. \\ \text{Non-trivial solution:} & \boldsymbol{\lambda} \text{ is not constant with respect to } \tau. \end{cases}$$

B.3 Ordinary, limit, and bifurcation points

With reference to the eigenvalues e_i $(i = 1, \dots, n)$ of the Jacobian matrix J, equilibrium points are classified as

$$\begin{cases} e_i \neq 0 \text{ for all } i, & \text{ordinary point,} \\ e_i = 0 \text{ for some } i, & \text{critical (singular) point.} \end{cases}$$

Critical points are classifiable as

$$\begin{cases} \text{limit point of } \tau \ (M = 1), \\ \text{bifurcation point} \begin{cases} \text{simple } (M = 1), \\ \text{double } (M = 2), \\ \qquad \vdots \end{cases} \end{cases}$$

where M is the multiplicity of a critical point that is defined as the number of zero eigenvalues of J.

At a limit point of τ, as portrayed in Fig. 11(a), the value of τ is maximized or minimized. A feasible path is shown by the solid curve, and an infeasible one by the dashed curve. Two half branches are connected at the

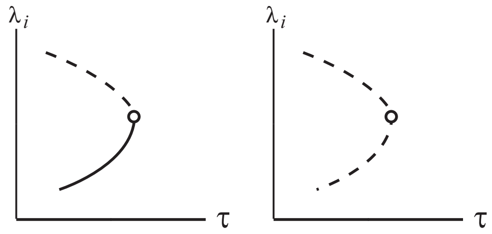

(a) Limit point of τ

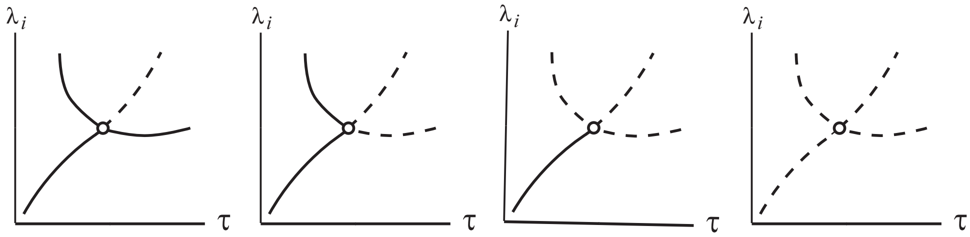

(b) Bifurcation point

Figure 11: Critical points (solid curve, feasible; dashed curve, infeasible)

limit point; a part of the path beyond the limit point is called a *half branch* and so is another part. With regard to economical feasibility, there are two cases:

- A half branch is feasible, but another half branch is not.
- Both half branches are infeasible.

At a bifurcation point, two or more equilibrium paths intersect: Fig. 11(b) presents a simple bifurcation point at which two paths (four half branches) intersect. With regard to economical feasibility, there are four cases: Three, two, one, or zero half branches are feasible, and the remaining half branches are infeasible. If we focus only on feasible half branches, they look like a two-pronged weapon, a curve with a kink, a branch, and so on.

B.4 Break and sustain points

Recall the block-diagonal form (15) in §4:

$$\tilde{J} = H^\top J H = \begin{pmatrix} \tilde{J}^0 & & O \\ & \tilde{J}^1 & \\ O & & \ddots \end{pmatrix}.$$

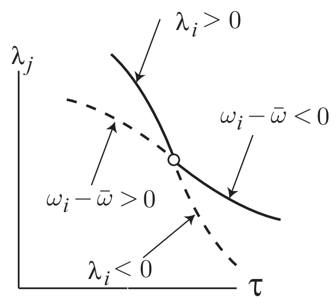

(a) Crossing point of two non-trivial solutions

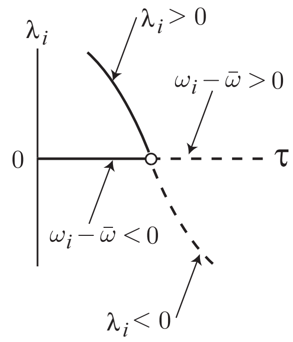

(b) Crossing point of trivial and non-trivial solutions

Figure 12: Sustain points (solid curve, feasible; dashed curve, infeasible)

At a bifurcation point, a block $\tilde{J}^k$ for some k becomes singular. Depending on the type of block that becomes singular, bifurcation points are classified into two types:

- A *break bifurcation point*, or a break point, is symmetry-breaking one, at which $\tilde{J}^k$ becomes singular for some $k(\geq 1)$. The symmetry of the system is reduced on a bifurcated path branching at a break point (cf. §5).
- A *sustain bifurcation point*, or a sustain point is a symmetry-preserving one, at which $\tilde{J}^0$ becomes singular. The symmetry of the system is preserved on a bifurcated path branching at a sustain point.

The sustain bifurcation point is an inherent feature of the present core–periphery model that permits the extinction of city population of manufacturing labor. This point is necessarily a bifurcation point because the factorized form $(\omega_i - \bar{\omega})\lambda_i$ of (10) (cf. Remark 1) produces two independent solutions. The point, as shown in Fig. 12, is classified into two types[24]: (a) the crossing point of two non-trivial solutions and (b) the crossing point of a trivial solution and a non-trivial solution.

[24]The sustain point for the two cities in Fujita et al. (1999) [10] corresponds to the crossing point of a trivial solution and a non-trivial solution in Fig. 12(b).

Since λ_i and $\omega_i - \bar{\omega}$ vanish simultaneously at this point, the sign of $\omega_i - \bar{\omega}$ along a (trivial) solution path changes, as does the sign of λ_i along another path. At the point, a sustainable solution ($\omega_i - \bar{\omega} < 0$, $\lambda_i = 0$) changes into an unsustainable one ($\omega_i - \bar{\omega} > 0$, $\lambda_i = 0$) along a path, while a feasible solution with positive population ($\lambda_i > 0$, $\omega_i - \bar{\omega} = 0$) changes into an infeasible one with negative population ($\lambda_i < 0$, $\omega_i - \bar{\omega} = 0$).

Remark 3 Fujita et al. (1999) [10] considered only feasible solutions, and regarded the sustain point as a kink that connect two half branches. Yet this point is considered as a bifurcation point in this paper to be consistent with the computational bifurcation theory in Appendix E.

C Proofs

Proof of Proposition 1. The Jacobian matrix of the equality condition (10) reads

$$\begin{aligned} J &= \frac{\partial \boldsymbol{F}}{\partial \boldsymbol{\lambda}} \\ &= \begin{pmatrix} \omega_1 - \bar{\omega} & 0 & \cdots & 0 \\ 0 & \omega_2 - \bar{\omega} & \ddots & \vdots \\ \vdots & \ddots & \ddots & 0 \\ 0 & \cdots & 0 & \omega_n - \bar{\omega} \end{pmatrix} + \begin{pmatrix} \Omega_{11}\lambda_1 & \Omega_{12}\lambda_1 & \cdots & \Omega_{1n}\lambda_1 \\ \Omega_{21}\lambda_2 & \Omega_{22}\lambda_2 & \ddots & \vdots \\ \vdots & \ddots & \ddots & \vdots \\ \Omega_{n1}\lambda_n & \cdots & \cdots & \Omega_{nn}\lambda_n \end{pmatrix} \\ &= \mathrm{diag}(\omega_1 - \bar{\omega}, \ldots, \omega_n - \bar{\omega}) + \mathrm{diag}(\lambda_1, \ldots, \lambda_n)\Omega, \end{aligned} \tag{C.1}$$

where $\mathrm{diag}(\cdots)$ denotes a diagonal matrix with diagonal entries therein and

$$\Omega_{ij} = \frac{\partial(\omega_i - \bar{\omega})}{\partial \lambda_j}, \quad (i, j = 1, \ldots, n), \tag{C.2}$$

$$\Omega = (\Omega_{ij} \mid i, j = 1, \ldots, n). \tag{C.3}$$

For an interior solution with $\omega_i - \bar{\omega} = 0$ and $\lambda_i > 0$ ($i = 1, \ldots, n$) (cf. (5) and Appendix B.1), the Jacobian matrix in (C.1) reduces to

$$J = \mathrm{diag}(\lambda_1, \ldots, \lambda_n)\Omega. \tag{C.4}$$

An interior solution is stable if all the eigenvalues of the matrix Ω in (C.3) have negative real parts (cf. §3.2) because the matrix $\mathrm{diag}(\lambda_1, \ldots, \lambda_n)$ in (C.4) is positive definite.

A corner solution (cf. Appendix B.1) can be expressed without loss of generality[25] as

$$\lambda_i > 0,\ \omega_i - \bar{\omega} = 0, \qquad (i = 1, \ldots, m), \tag{C.5}$$

$$\lambda_i = 0, \qquad (i = m+1, \ldots, n). \tag{C.6}$$

With the use of (C.5), the Jacobian matrix in (C.1) becomes

$$J = \left(\begin{array}{c|ccc} \Phi_1 & & \Phi_2 & \\ \hline & \omega_{m+1} - \bar{\omega} & & 0 \\ O & & \ddots & \\ & 0 & & \omega_n - \bar{\omega} \end{array}\right), \tag{C.7}$$

where

$$\Phi_i = \mathrm{diag}(\lambda_1, \ldots, \lambda_m)\Omega_i, \quad (i = 1, 2),$$

$$\Omega_1 = \begin{pmatrix} \Omega_{11} & \cdots & \Omega_{1m} \\ \vdots & \ddots & \vdots \\ \Omega_{m1} & \cdots & \Omega_{mm} \end{pmatrix}, \quad \Omega_2 = \begin{pmatrix} \Omega_{1(1+m)} & \cdots & \Omega_{1n} \\ \vdots & \ddots & \vdots \\ \Omega_{m(1+m)} & \cdots & \Omega_{mn} \end{pmatrix}.$$

From (C.7), it is apparent that $e_i = \omega_i - \bar{\omega}$ $(i = m+1, \ldots, n)$ are eigenvalues of J, whereas the other m eigenvalues e_i $(i = 1, \ldots, m)$ are given as eigenvalues of Φ_1.

For a stable corner solution, we have $e_i = \omega_i - \bar{\omega} < 0$ $(i = m+1, \ldots, n)$, whereas $\omega_i - \bar{\omega} = 0$ $(i = 1, \ldots, m)$ by (C.6). Therefore, the sustainability $\omega_i - \bar{\omega} \leq 0$ $(i = 1, \ldots, n)$ in (5) is satisfied for the stable solution. Consequently, the check of the sustainability is to be replaced with the investigation of stability. $\square$

[25] The consideration of this form does not lose generality because all corner solutions can be reduced to the form by appropriately rearranging the order of independent variables $\boldsymbol{\lambda}$.

Proof of Lemma 1. With the use of the representation matrices for $c(2\pi/n)$ and σ:

$$T(c(2\pi/n)) = \begin{pmatrix} & & & 1 \\ 1 & & & \\ & \ddots & & \\ & & 1 & \end{pmatrix}, \quad T(\sigma) = \begin{pmatrix} 1 & & & \\ & & & 1 \\ & & \iddots & \\ & 1 & & \end{pmatrix},$$

the representation matrices $T(g)$ $(g \in \mathrm{D}_n)$ can be generated as

$$T(c(2\pi i/n)) = \{T(c(2\pi/n))\}^i, \quad T(\sigma c(2\pi i/n)) = T(\sigma)\{T(c(2\pi/n))\}^i,$$

$(i = 0, 1, \ldots, n-1)$.

In the proof of the equivariance (17), we note that

$$\bar{\omega}(T(g)\boldsymbol{\lambda}, \tau) = \bar{\omega}, \quad \boldsymbol{\omega}(T(g)\boldsymbol{\lambda}, \tau) = T(g)\boldsymbol{\omega}(\boldsymbol{\lambda}, \tau),$$

where the former denotes the objectivity of $\bar{\omega}$ with respect to the numbering of cities, and the latter denotes that the rearrangement of $\boldsymbol{\lambda}$ leads to the rearrangement of $\boldsymbol{\omega}$ in the same order. Then, for example, for $g = \sigma$

$$\begin{aligned} \boldsymbol{F}(T(\sigma)\boldsymbol{\lambda}, \tau) &= \begin{pmatrix} \{\omega_1(T(\sigma)\boldsymbol{\lambda}, \tau) - \bar{\omega}(T(\sigma)\boldsymbol{\lambda}, \tau)\}\lambda_1 \\ \{\omega_2(T(\sigma)\boldsymbol{\lambda}, \tau) - \bar{\omega}(T(\sigma)\boldsymbol{\lambda}, \tau)\}\lambda_n \\ \{\omega_3(T(\sigma)\boldsymbol{\lambda}, \tau) - \bar{\omega}(T(\sigma)\boldsymbol{\lambda}, \tau)\}\lambda_{n-1} \\ \vdots \\ \{\omega_n(T(\sigma)\boldsymbol{\lambda}, \tau) - \bar{\omega}(T(\sigma)\boldsymbol{\lambda}, \tau)\}\lambda_2 \end{pmatrix} \\ &= \begin{pmatrix} \{\omega_1(\boldsymbol{\lambda}, \tau) - \bar{\omega}(\boldsymbol{\lambda}, \tau)\}\lambda_1 \\ \{\omega_n(\boldsymbol{\lambda}, \tau) - \bar{\omega}(\boldsymbol{\lambda}, \tau)\}\lambda_n \\ \{\omega_{n-1}(\boldsymbol{\lambda}, \tau) - \bar{\omega}(\boldsymbol{\lambda}, \tau)\}\lambda_{n-1} \\ \vdots \\ \{\omega_2(\boldsymbol{\lambda}, \tau) - \bar{\omega}(\boldsymbol{\lambda}, \tau)\}\lambda_2 \end{pmatrix} \\ &= T(\sigma)\boldsymbol{F}(\boldsymbol{\lambda}, \tau). \end{aligned}$$

This shows the equivariance (17) for $g = \sigma$. The equivariance for other elements of $g \in \mathrm{D}_n$ can be shown similarly. $\square$

Proof of Proposition 2. We consider D_m-symmetric state, for which the equivariance (13) with $G = \mathrm{D}_m$ for the explicit form of $\boldsymbol{F}$ in (10) entails

$$\begin{aligned} &\omega_1 = \omega_{1+n/m} = \cdots = \omega_{1+(m-1)n/m}, \\ &\omega_2 = \omega_{2+n/m} = \cdots = \omega_{2+(m-1)n/m}, \\ &\quad\vdots \\ &\omega_{n/m} = \omega_{2n/m} = \cdots = \omega_n. \end{aligned} \tag{C.8}$$

As a candidate for a trivial solution, we consider a D_m-symmetric population distribution

$$\begin{cases} \lambda_i = 1/m, \ \omega_i - \bar{\omega} = 0, & (i = 1, 1+n/m, \ldots, 1+(m-1)n/m), \\ \lambda_i = 0, & \text{otherwise}, \end{cases} \tag{C.9}$$

which is obtained by setting $k = 1$ in (19).

The substitution of (C.9) into (10) yields

$$\boldsymbol{F} = \begin{pmatrix} \{\omega_1 - \bar{\omega}\}\lambda_1 \\ \vdots \\ \{\omega_n - \bar{\omega}\}\lambda_n \end{pmatrix} = \begin{pmatrix} 0 \times \lambda_1 \\ (\omega_2 - \omega_1) \times 0 \\ \vdots \\ (\omega_{n/m} - \omega_1) \times 0 \\ \vdots \end{pmatrix} = \mathbf{0}.$$

This proves that (C.9) is a trivial solution, while other trivial solutions are treated similarly. □

Proof of Proposition 4. The critical eigenvector is given by the superposition of the two vectors $\boldsymbol{\eta}^{(j),1}$ and $\boldsymbol{\eta}^{(j),2}$ in (23) as

$$\boldsymbol{\eta}(\theta) = \cos\theta \cdot \boldsymbol{\eta}^{(j),1} + \sin\theta \cdot \boldsymbol{\eta}^{(j),2}$$

for general angle θ ($0 \leq \theta < 2\pi$). The bifurcated paths do not branch in the general direction associated with arbitrary θ, but branch in finite directions as expounded in Lemma 2. This is a novel aspect presented in this paper that was not examined for the core–periphery model up to now.

Lemma 2 *As made clear by group-theoretic analysis (cf. Ikeda et al., 1991 [17]; Ikeda and Murota, 2002 [16]), bifurcated paths branching at the double bifurcation point satisfy the following properties:*

(i) *There exist* $\widehat{n}$ *bifurcated paths (*$2\widehat{n}$ *half branches) in the directions of*

$$\delta\boldsymbol{\lambda} = C\boldsymbol{\eta}(\alpha_k),\ C\boldsymbol{\eta}(\alpha_{k+\widehat{n}}), \quad (k = 1, \ldots, \widehat{n}),$$

where C *is a scaling constant and*

$$\alpha_i = -\pi\ (i-1)/\widehat{n}, \quad (i = 1, \ldots, 2\widehat{n}).$$

(ii) *The solutions* $\delta\boldsymbol{\lambda} = C\boldsymbol{\eta}(\alpha_k)$ *and* $C\boldsymbol{\eta}(\alpha_{k+\widehat{n}})$ *are* $\mathrm{D}^{k,n}_{n/\widehat{n}}$*-symmetric* ($k = 1, \ldots, \widehat{n}$). *Therefore, the spatial period becomes* $\widehat{n}$*-times* ($\widehat{n} \geq 3$) *in comparison with that of the* D_n*-symmetric uniform population solution.*

(iii) *The* $2\widehat{n}$ *half branches are classifiable into two independent ones:* $\delta\boldsymbol{\lambda} = C\boldsymbol{\eta}(\alpha_{2l-1})$, $C\boldsymbol{\eta}(\alpha_{2l})$ ($l = 1, \ldots, \widehat{n}$). *It suffices in numerical analysis to find the two branches in two directions:* $\delta\boldsymbol{\lambda} = C\boldsymbol{\eta}(\alpha_1)$, $C\boldsymbol{\eta}(\alpha_2)$.

□

Remark 4 Proposition 2 is extendible to double bifurcation points on bifurcated paths with D_m-symmetry (m divides n; $m \geq 3$) by choosing $\boldsymbol{\eta}^{(j),1}$ and $\boldsymbol{\eta}^{(j),2}$ to be $\mathrm{D}^{1,m}_{m/\widehat{m}}$- and $\mathrm{D}^{1+\widehat{m}/2,m}_{m/\widehat{m}}$-symmetric, respectively. Here $\widehat{m} = m/\gcd(j, m)$ and $1 \leq j < m/2$.

D Hierarchical bifurcations

We explain the mechanism of hierarchical bifurcations of the racetrack economy that consist of symmetry-breaking at break points and the extinction of city population of manufacturing labor at sustain points, en route to the concentration of population in a city. As mentioned in Appendix B.4, these points are characterized by

$$\begin{cases} \text{break point:} & \text{symmetry breaking,} \\ \text{sustain point:} & \text{symmetry preserving.} \end{cases}$$

D.1 Break bifurcations

In addition to break bifurcations from the uniform-population trivial solution with D_n-symmetry that were studied in §5.3, there are several possible sources of symmetry-breaking. Namely, further break bifurcations may be encountered on (a) bifurcated paths of this D_n-symmetric solution and (b) D_m-symmetric trivial solutions (m divides n) presented in §5.2.

All these break bifurcations can be described by group-theoretic bifurcation theory (cf. Ikeda and Murota, 2002 [16]). The rule of bifurcation depends on the integer number n. To be precise, it depends on the divisors of the number n, and the bifurcation becomes increasingly hierarchical and complex for n with more divisors.

A few examples are:

- If n is a prime number, then it can undergo the one and only course of hierarchical bifurcations: $\mathrm{D}_n \longrightarrow \mathrm{D}_1 \longrightarrow \mathrm{C}_1$.

- For $n = 4 = 2^2$, a hierarchy of subgroups expressing the rule of hierarchical break bifurcations is presented in Fig. 13(a). As might be readily apparent, in addition to the direct bifurcations in Fig. 5, several secondary and tertiary bifurcations exist: D_2-symmetric solution branches into $\mathrm{D}_1^{k,4}$-symmetric ones ($k = 1, \ldots, 4$) and $\mathrm{D}_1^{k,4}$-symmetric one branches into C_1-symmetric one.

- The hierarchy of subgroups for $n = 6 = 2 \times 3$ shown in Fig. 13(b) portrays a more complex hierarchy than that of $n = 4 = 2^2$ in Fig. 13(a).

These rules are sufficient in the description for break bifurcations of the model, while the model in general undergoes more complex bifurcation due to the presence of sustain bifurcation points as explained in Appendix D.2.

D.2 Sustain bifurcations

As mentioned in Appendix B.4, the sustain bifurcation point is a special feature of the core–periphery model that leads to the extinction of city population of manufacturing labor. If we follow only feasible solutions, we must switch into another feasible path. A sustain point may possibly appear in

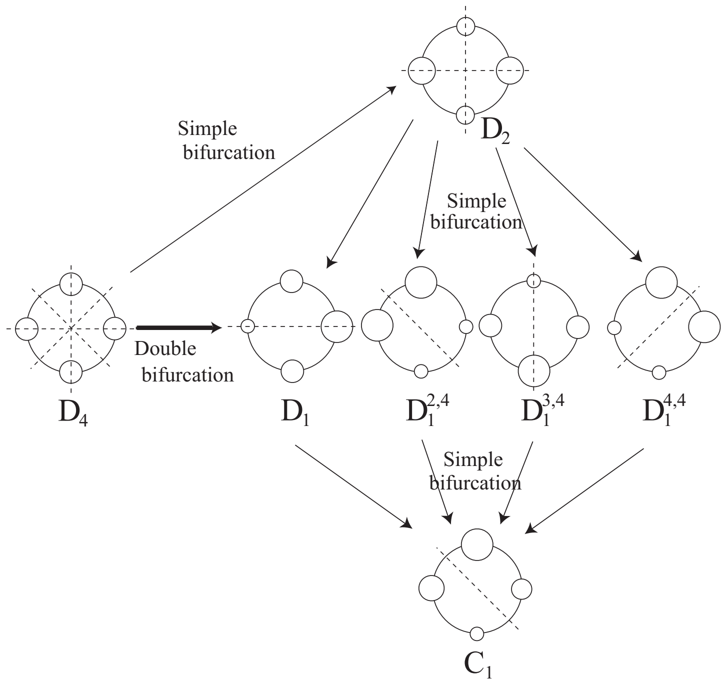

(a) Four cities ($n = 4$)

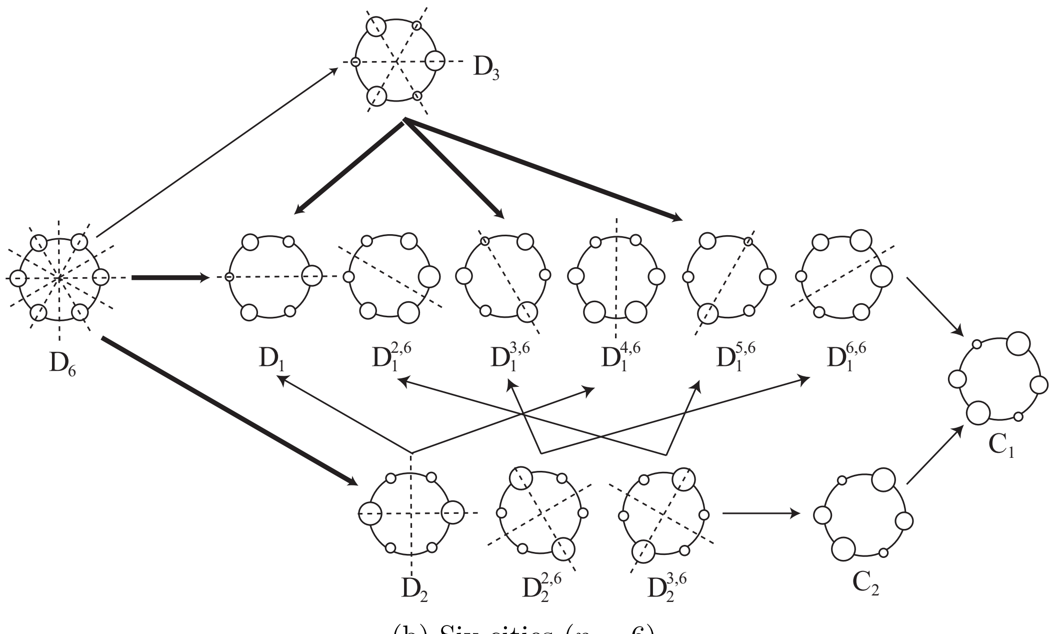

(b) Six cities ($n = 6$)

Figure 13: Hierarchy of subgroups associated with hierarchical break bifurcations (dark solid arrow, double bifurcation; thin solid arrow, simple bifurcation)

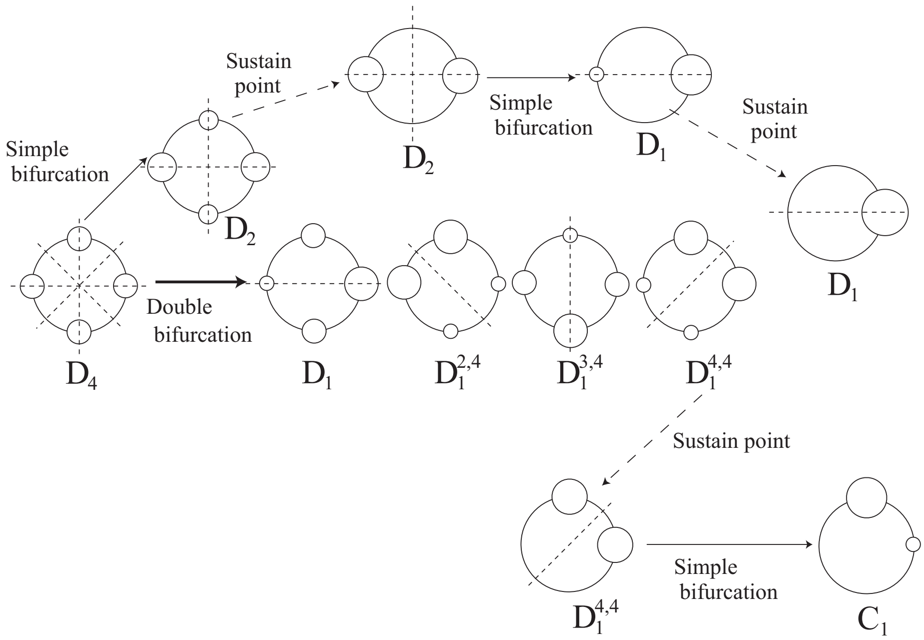

Figure 14: Hierarchical, break and sustain bifurcations of the four cities ($n = 4$; solid arrow, break bifurcation; dashed arrow, sustain bifurcation)

any solutions other than the uniform population solution. The presence of sustain bifurcation points must be meshed into the rule of break bifurcations presented in Appendix D.1.

A possible course of hierarchical bifurcations is presented in Fig. 14, for example, for the four cities ($n = 4$). From the trivial solution with uniform population ($\boldsymbol{\lambda} = (1/4, 1/4, 1/4, 1/4)^\top$) shown in the left, population distribution patterns of various kinds are engendered via hierarchical bifurcations. In this figure, we encounter sustain bifurcation points shown by the dashed arrows, in addition to the double bifurcation shown by the dark solid arrow and the simple bifurcations shown by the thin solid arrows. Cases other than $n = 4$ can be treated similarly.

E Computational bifurcation theory

As we will see in §6, the solutions of the governing equation of the racetrack economy involve several bifurcated paths that are quite complex. These paths can be traced in a systematic and exhaustive manner by computational bifurcation theory (cf. Crisfield, 1977 [5]). To be concrete, we employ the following three numerical steps:

- *Path tracing*: In the path tracing of non-trivial solutions, we refer to the incremental form of the equality equation (10), i.e.

$$\begin{aligned} &\boldsymbol{F}(\boldsymbol{u}+\delta\boldsymbol{u},\tau+\delta\tau)-\boldsymbol{F}(\boldsymbol{\lambda},\tau) \\ &= J(\boldsymbol{\lambda},\tau)\delta\boldsymbol{\lambda}+\frac{\partial\boldsymbol{F}}{\partial\tau}(\boldsymbol{\lambda},\tau)\ \delta\tau+\text{h.o.t.}=\boldsymbol{0}, \end{aligned} \tag{E.1}$$

  where h.o.t. denotes higher order terms. At each equilibrium point $(\boldsymbol{\lambda},\tau)$, another equilibrium point $(\boldsymbol{\lambda}+\delta\boldsymbol{\lambda},\tau+\delta\tau)$ can be found by solving[26] (E.1) for $(\delta\boldsymbol{\lambda},\delta\tau)$ using a predictor–corrector (Newton–Raphson) type method.

  For the trivial solution(s), we need not carry out path tracing because they are obtainable simply by symmetry consideration (cf. §5.2), although singularity detection and branch switching must be conducted.

- *Singularity detection*: We carry out the eigenanalysis of the Jacobian matrix $J(\boldsymbol{\lambda},\tau)$ at the solutions $(\boldsymbol{\lambda},\tau)$ to find the location of a critical point, as a point at which one or more eigenvalues e_i of $J(\boldsymbol{\lambda},\tau)$ become zero.

  For the uniform population solutions, the eigenanalysis can be conducted using the explicit formulas in (22)$\sim$(27). For the other solutions, the numerical eigenanalysis of J, which is in general a non-symmetric matrix, must be conducted.

- *Branch switching*: To obtain bifurcated paths branching from a bifurcation point, we use the so-called line search method.

[26]In the incremental equation (E.1), $(\boldsymbol{\lambda},\tau)$ is fixed, $\delta\boldsymbol{\lambda}$ is treated as an independent variable, and $\delta\tau$ as a bifurcation parameter.

At a simple bifurcation point with a single zero eigenvalue, say $e_1{=}0$ ($M{=}1$), a bifurcated path is to be sought in the direction of the critical eigenvector $\boldsymbol{\eta}_1$ associated with this zero eigenvalue. We employ $\delta\boldsymbol{\lambda} = C\boldsymbol{\eta}_1$ as the initial value for the iteration to find a solution on a bifurcated path, where the scaling constant C is to be specified pertinently in view of the convergence of the iteration.

At a double bifurcation point with two zero eigenvalues, say $e_1 = e_2 = 0$ ($M{=}2$), two (independent) bifurcated paths are to be sought in the directions $\delta\boldsymbol{\lambda} = C\boldsymbol{\eta}(\alpha_1)$ and $C\boldsymbol{\eta}(\alpha_2)$ in Proposition 2(iii).

We carry out an *exhaustive search* of a whole set of equilibrium paths of the racetrack economy by repeating the three steps described above for secondary, tertiary, ... bifurcated paths, until exhaustion of possible bifurcated paths.

For the racetrack economy, it is possible to trace trivial solutions independently, other than the uniform population solution, and to find bifurcated paths from these trivial solutions (cf. §5.5).